

# **ELECTRONIC RELAXATION AND DISSIPATION IN MESOSCOPIC SYSTEMS**

**THÈSE N° 2204 (2000)**

**PRÉSENTÉE AU DÉPARTEMENT DE PHYSIQUE**

**ÉCOLE POLYTECHNIQUE FÉDÉRALE DE LAUSANNE**

**POUR L'OBTENTION DU GRADE DE DOCTEUR ÈS SCIENCES**

**PAR**

**Kamran HOUSHANG POUR ISLAM**

**Diplom-Physiker, Johann Wolfgang Goethe-Universität, Frankfurt A.M. Allemagne  
de nationalité iranienne**

**acceptée sur proposition du jury:**

**Dr K. Maschke, directeur de thèse  
Prof. J.-Ph. Ansermet, rapporteur  
Prof. H. Beck, rapporteur  
Prof. F. Rossi, rapporteur**

**Lausanne, EPFL  
2000**

## Version Abrégée

Cette thèse s'inscrit dans le cadre de l'étude théorique du transport électronique dans de petits conducteurs à basses températures. Notre but est de comprendre l'interaction entre les systèmes mésoscopiques et l'environnement statistique, et ses effets sur les dispositifs électroniques dans le domaine du transport. Dans une première approche basée sur la description du transport de Landauer, nous étudions de manière phénoménologique les propriétés du transport d'un échantillon mésoscopique relié à des réservoirs électroniques. En particulier, nous nous intéressons à l'influence du couplage à l'environnement statistique sur le temps de cohérence de phase et à la conductibilité d'un système électronique ouvert. Nos résultats ont pu expliquer les données expérimentales récentes montrant la saturation du temps de cohérence de phase à basses températures et l'apparition des plateaux non universels de conductibilité dans les fils quantiques parfaits.

Nous présentons un modèle microscopique en assurant le couplage entre un petit système électronique fini et son environnement par l'intermédiaire de degrés de liberté vibratoires locaux. En appliquant une simple méthode itérative, nous calculons l'évolution temporelle de la matrice de densité du système.

En nous basant sur ces idées, nous étudions la relaxation d'énergie électronique dans un anneau unidimensionnel, et nous discutons le rôle de l'interaction d'électron-électron et du couplage à l'environnement. Nous analysons les courants dans un anneau traversé par un flux magnétique constant, et nous comparons nos résultats à la théorie habituelle de l'état fondamental pour les courants permanents.

Notre modèle est étendu à la description de l'évolution temporelle de la matrice de densité des électrons dans un anneau traversé par un champ magnétique dépendant du temps. En particulier, nous étudions la dynamique du système en présence ainsi qu'en absence de dissipation. Dans cette description, les processus cohérents et dispersifs sont uniformément distribués sur l'anneau, alors que dans l'approche de Landauer au courant continu dissipatif, les régions dispersives et cohérentes sont séparées spatialement.

---

**Mots clés:** Systèmes mésoscopiques, propriétés électroniques, dissipation, relaxation énergétique, goulots d'étranglement, courants persistants.



## Abstract

This thesis is concerned with the theoretical study of the transport in small conductors at low temperatures. Our aim is to elucidate the interplay between the statistical environment and mesoscopic systems, and its effect on electronic features in the domain of transport. In a first phenomenological approach based on the Landauer picture of transport, we study dc transport properties of a mesoscopic sample connected to electronic reservoirs. The influence of the coupling to the statistical environment on the phase-coherence time and on the conductance of an electronic open system is then investigated. Our results may explain recent experimental findings showing the saturation of the phase-coherence time at low temperatures and the emergence of nonuniversal conductance steps in perfect quantum wires.

We present a microscopic model to account for the coupling between small finite electronic systems and the further environment via local vibrational degrees of freedom. We calculate the time-evolution of the density matrix of the sample system, by applying a simple iterative procedure.

Using this approach, the energy relaxation of electrons in a one-dimensional loop is studied and the role of the electron-electron interaction and the coupling to the environment is discussed.

We analyse currents in a loop, which is threaded by a constant magnetic flux, and compare our results with the common ground state theory of the persistent currents.

Our model is extended to describe the situation of a loop, in which the electrons are driven by a time-dependent magnetic field. In particular, we study the electronic current in the presence as well as in the absence of dissipation. In this description, both coherent and dissipative processes are uniformly distributed in the loop system, in contrast with the Landauer approach to dc transport, where dissipative and coherent regions are spatially separated.

---

**Keywords:** Mesoscopic systems, electronic properties, dissipation, energy relaxation, bottlenecks, persistent currents.



## Zusammenfassung

Diese Arbeit befaßt sich mit der theoretischen Beschreibung des Elektronentransports in kleinen Proben bei tiefen Temperaturen. Unser Ziel ist, das Zusammenspiel zwischen mesoskopischen Systemen und der statistischen Umgebung sowie deren Einfluß auf die elektronischen Transporteigenschaften zu erläutern. Ausgehend von der Landauer Theorie betrachten wir zunächst die Gleichstromeigenschaften einer an zwei elektronische Reservoirs angeschlossenen mesoskopischen Probe. Der Einfluß der statistischen Umgebung auf die Phasenkohärenzzeit und auf den Leitwert eines elektronisch offenen Systems wird untersucht. Unsere Resultate liefern eine mögliche Erklärung für die experimentell beobachtete Sättigung der Phasenkohärenzzeit bei niedrigen Temperaturen sowie das Auftreten von nichtuniversellen Leitwertstufen in perfekten Quantendrähten.

Des weiteren schlagen wir ein mikroskopisches Modell vor, das uns erlaubt, die Kopplung zwischen kleinen begrenzten elektronischen Systemen und ihrer Umgebung über lokale Schwingungsfreiheitsgrade zu beschreiben. Wir berechnen die Zeitentwicklung der Dichtematrix des Systems mit Hilfe einer einfachen Iterationstechnik.

Diese Methode ermöglicht es uns, die Energierelaxation der Elektronen in einer eindimensionalen Schleife, als auch die Rolle der Elektron-Elektron-Wechselwirkung und der Kopplung zur Umgebung zu behandeln.

Wir analysieren die Dauerströme in einer Schleife in einem konstanten Magnetfeld und vergleichen unsere Ergebnisse mit denen der üblichen Grundzustandstheorie.

Unser Modell gibt uns weiter die Möglichkeit, die Dynamik der durch ein zeitabhängiges Magnetfeld angetriebenen Elektronen in einem Ring zu beschreiben. Insbesondere untersuchen wir den Einfluß dissipativer Streuung auf den Strom. In diesem Fall sind kohärente sowie dissipative Prozesse gleichmäßig auf dem Ringsystem verteilt, im Gegensatz zum Landauer-Bild, in dem dissipative und kohärente Regionen räumlich von einander getrennt sind.

---

**Schlagwörter:** Mesoskopische Systeme, elektronische Eigenschaften, Dissipation, Energierelaxation, Flaschenhalseffekte, Dauerströme



# Contents

---

<b>1</b>	<b>Introduction</b>	<b>8</b>
<b>2</b>	<b>General aspects</b>	<b>11</b>
2.1	Characteristic lengths . . . . .	12
2.1.1	Mean Free Path . . . . .	12
2.1.2	Fermi Wave Length . . . . .	12
2.1.3	Thermal Diffusion Length . . . . .	13
2.1.4	Phase-Coherence Length . . . . .	13
2.2	Landauer Picture of Transport . . . . .	14
2.2.1	Aspects of Landauer-Büttiker Approach . . . . .	16
2.3	Experimental Techniques . . . . .	18
2.3.1	Aharonov-Bohm Effect . . . . .	18
2.3.2	Weak Localization Regime . . . . .	19
<b>3</b>	<b>Dissipation in Electronically Open Systems</b>	<b>20</b>
3.1	Phase-Coherence Time at Low Temperatures . . . . .	21
3.1.1	Phase-Coherence Time in Presence of Electron-Phonon Scattering Processes . . . . .	22
3.1.2	Discussion and Suggestions for Further Investigations . . . . .	25
3.2	Nonuniversal Conductance Steps . . . . .	26
3.2.1	Model Description . . . . .	28
3.2.2	Rate Equations . . . . .	29
3.2.3	Energy Dependence of Level Occupation . . . . .	30
3.2.4	Comparison with Experiment and Predictions . . . . .	32
<b>4</b>	<b>Electron Relaxation in Small Systems</b>	<b>35</b>
4.1	Theoretical Model . . . . .	36
4.2	Single-Electron Relaxation in Small 1D Loops . . . . .	39
4.2.1	Numerical Results . . . . .	40
4.3	Two-Electron Relaxation . . . . .	46
4.3.1	Pauli Exclusion . . . . .	47

4.3.2	Electron-Electron Interaction . . . . .	48
<b>5</b>	<b>Persistent Currents</b>	<b>53</b>
5.1	Persistent Currents in the Electronic Ground State . . . . .	54
5.2	Persistent Currents in Presence of Environmental Coupling . . . . .	56
5.3	Higher Harmonics . . . . .	59
5.3.1	Persistent Currents of Interacting Electrons . . . . .	59
<b>6</b>	<b>Transport in Loops Coupled to Their Environment</b>	<b>61</b>
6.1	Sudden Approximation . . . . .	61
6.2	Bloch Oscillations in small two-electron loop systems . . . . .	63
6.2.1	Effects of Electron-Electron Interaction . . . . .	63
6.3	Damping of Bloch Oscillations and DC in Presence of Dissipation	66
<b>7</b>	<b>Conclusions</b>	<b>68</b>
<b>A</b>	<b>Electronic Arrays</b>	<b>71</b>
A.1	Two-Electron States . . . . .	71
A.2	Calculation of Electron-Electron Interaction on Loops . . . . .	72

# List of Figures

---

2.1	Aharonov-Bohm ring . . . . .	13
2.2	Two-terminal device . . . . .	15
3.1	Temperature dependence of the phase-coherence time . . . . .	24
3.2	Fits to the measured values of the phase-coherence time . . . . .	25
3.3	Two-level transport picture . . . . .	28
3.4	Nonuniversal conductance step . . . . .	32
4.1	Model illustration of coupling to the environment . . . . .	36
4.2	Single-electron relaxation . . . . .	41
4.3	Single-electron occupation at different times . . . . .	42
4.4	$\tau_p$ -dependence of the stationary state . . . . .	43
4.5	$\omega$ -dependence of the stationary state . . . . .	44
4.6	Energy relaxation of an electron coupled to acoustical modes . . .	45
4.7	State occupation of an electron coupled to acoustical modes . . .	46
4.8	Two non-interacting electrons . . . . .	48
4.9	Relaxation of two weakly interacting electrons with parallel spins	49
4.10	Relaxation of two weakly interacting electrons with opposite spins	50
4.11	Relaxation of two interacting electrons with parallel spins . . . . .	51
4.12	Energy eigenvalues of a two-electron system for different interaction parameters . . . . .	51
4.13	Stationary state of relaxing system for two different initial states .	52
5.1	Persistent currents of non-interacting electrons . . . . .	55
5.2	Persistent currents of interacting electrons in tight-binding model	55
5.3	Persistent currents of electrons in a loop coupled to the environment	57
5.4	$\omega$ -dependence of persistent currents . . . . .	58
5.5	Persistent currents of interacting electrons in a loop coupled to the environment . . . . .	60
6.1	Bloch oscillations of a coherent driven system . . . . .	64
6.2	Quantum beats of interacting electrons . . . . .	65

6.3	Damped Bloch oscillations for non-interacting electrons . . . . .	66
6.4	Damped beats for interacting electrons coupled to the environment	67
A.1	Two electrons in a tight-binding band . . . . .	71
A.2	Distance between two sites <i>on</i> a loop . . . . .	72

# Chapter 1

## Introduction

---

The rapid progress of device technology in the past two decades has drastically changed the focus of fundamental research in the domain of electronic transport. Historically, interference effects were first considered in the description of transport in disordered solids [1, 2, 3, 4]. The experimental realization of a two-dimensional electron gas at low temperatures was a first step towards a new transport regime, which got the denomination “mesoscopic”. Small conductors whose dimensions are intermediate between the microscopic and the macroscopic ones, are called mesoscopic from the greek “mesos”, which means “between”. The dimensions of these samples are comparable to the coherence length of the carriers so that the quantum behavior of the carriers affects their transport properties. The experimental evidence for phenomena like the quantum Hall effect, universal conductance fluctuations, non-dissipative direct currents (so-called persistent currents), and Bloch oscillations have given evidence for the limitation of classical and semi-classical pictures of the dc transport. Soon after, it was realized that the transmission approach—a well-developed tool at the inception of quantum mechanics—offers an appropriate theoretical instrument to describe the dc transport properties of mesoscopic systems.

Phase coherence is a crucial concept for the understanding of mesoscopic systems. Due to their characteristic of being weakly coupled to the *statistical* environment, mesoscopic systems represent a convenient tool to study the onset of relaxation. In general, there are two types of experimental approaches:

- Optics. Experimentally accessible effects take place at a short time scale of the order pico seconds. Over short time scales, one can describe the dynamical behavior of the carriers in a mesoscopic sample system by the coherent evolution of the isolated system.
- Transport. The time scale for observable transport phenomena is rather long, so that the coupling between the sample and the further environment

has to be taken into account, since the phase coherence in the sample is gradually lost due to inelastic scattering processes induced by the statistical environment. In this work we focus on the transport properties of mesoscopic systems.

From the theoretical point of view, one can describe optical phenomena by solving the generalized Semiconductor-Bloch equations that account for the relevant quantum mechanical interactions [5, 6]. There are two main approaches to describe the transport features of mesoscopic systems. One of them is the Green's function approach, involving the Keldysh formalism [7]. Based on this description, Pötz has recently derived generalized Boltzmann-Bloch equations to study coherent carrier dynamics and phase breaking in mesoscopic semiconductor structures [8]. Datta has represented the environment by a continuum of local harmonic oscillators in thermal equilibrium that are coupled to the electronic subsystem [9].

In the description of dc transport developed by Landauer [1], the environment is accounted for by two statistically independent electron reservoirs, which are held at different chemical potentials to drive the current through the sample. Exploiting this idea, Büttiker recognized that dissipation in the sample can be phenomenologically simulated by means of fictitious voltage probes that are connected to additional electron reservoirs and satisfy the condition of current conservation [10]. The reservoirs are held at thermal equilibrium, so that the electrons are dissipated when entering one or more of the voltage probes. This approach has been successfully used to describe the onset of dissipation in the electronic dc transport in mesoscopic samples [11, 12, 13]. However, the need for a rigorous microscopic approach to dissipation still persists.

While phase-destroying processes are expected to vanish at temperatures  $T \rightarrow 0$  in closed systems [14], recent experiments have shown instead that the phase-coherence time saturates at low temperatures [15]. This result raised the question about the existence and the origin of dephasing processes at low temperatures, which has not yet been satisfactorily answered.

Almost at the same time, the experimental results presented by Yacoby *et al.* [16] posed another theoretical challenge to the scientific community. The authors of Ref. [16] studied the transport properties of perfect quantum wires at low temperatures and found measurable deviations in the conductance plateaus from the expected universal value of  $2e^2/h$ . The experiment showed that the step height of the conductance plateaus increases toward the universal value with the width of the wire, with the temperature and with the external bias. These authors argued that nonuniversal conductance steps can be explained neither by elastic impurities nor in terms of electron-electron interactions.

The role of electron-phonon interactions in electronic relaxation processes has been discussed by a number of authors. In particular, recent investigations on the so-called “phonon bottleneck”, which has been claimed to inhibit the cooling of carriers in quantum dots when the level separation does not match the phonon energy, have excited controversial points of view. The debates on this subject persist within both the theoretical and experimental communities [17, 18, 19].

In the present work, we study the possible effects of the contacts and the coupling to the environment on the transport properties of a mesoscopic sample system. Furthermore, we investigate the electronic properties of an initially isolated small system that interacts with its environment via local vibrational degrees of freedom.

Chapter 2 provides a brief overview of the Landauer picture of dc transport at lower dimensions and introduces some experimental techniques to measure the phase-coherence length.

Chapter 3 treats in a phenomenological manner the role of the contacts on dc transport measurements within the framework of the Landauer approach. We show that both, the saturation of the phase-coherence time and nonuniversal conductance steps, may be due to electronic transitions induced by phonon emission. These transitions remain possible even at low temperatures in electronically open systems.

In Chapter 4, we introduce a simple model to study electronic properties of a small sample system, containing a finite number of electronic and local vibrational degrees of freedom. The influence of the environment is considered in a phenomenological manner by attributing a finite lifetime to the vibrational states.

The time evolution of the density matrix of the system is then calculated within our approach. We describe the energy relaxation of one- and two-electron systems for a loop geometry of the sample. We note that, in contrast with the Landauer approach where coherent and dissipative regions are spatially separated, dissipation is uniformly distributed in the loop system. The effects of electron-electron interactions on the electronic relaxation in small systems are discussed.

Based on this model description, Chapter 5 deals with persistent currents in a small loop that is threaded by a constant magnetic flux. The role of relaxation bottlenecks and of the Coulomb interaction between the electrons is investigated.

In Chapter 6, we apply our model to describe the time evolution of the density matrix of a loop, in which the electrons are driven by a time-dependent magnetic field. The current through the isolated loop is studied for both interacting and non-interacting electrons. We then illustrate the transition from coherent to dissipative dc regime. Finally, our conclusions are given in Chapter 7.



# Chapter 2

## General aspects

---

Mesoscopic systems have attracted much attention in our time. On the one hand, they have been very important for the progress of the device technology in the past decade and for the development of new instruments used in fundamental research as well as in our everyday's life. On the other hand, they are also interesting in themselves, as their characteristic dimensions are intermediate between the atomic and the macroscopic length scales. In particular, one may expect a better understanding of the transition from quantum to classical behavior by studying the physical properties of nano devices.

Quantum mechanics states that the wavefunction  $|\Psi\rangle$ , describing the state of a closed system, evolves according to the Schrödinger equation,

$$i\hbar \frac{d}{dt} |\Psi\rangle = H |\Psi\rangle. \quad (2.1)$$

Given an initial state  $|\Psi_i\rangle$  and the Hamiltonian  $H$  of the system at time  $t_0$ , its state at any arbitrary time  $t$  is determined by Eq. 2.1. If we measure an observable of the system at  $t$ , the question can be raised as to what the outcome will be. The Copenhagen interpretation was the first attempt to find a solution to this problem [20], although not very satisfactory. It is based on a suggestion of Niels Bohr, who argued that a classical device that decides about the single outcome among all possible results is necessary for a measurement. This implies a sharp border between classical and quantum mechanics and claims quantum theory not to be universal.

Even though the clue to solve the measurement problem was already known from the early days of quantum theory, it is only in the past three decades that people have recognized its importance for the transition from quantum to classical [21, 22, 23]. In fact, Eq. 2.1 is only applicable to closed systems which evolve coherently as long as they are completely isolated from the *environment*. The interaction between the sample system and its environment causes *decoherence*

within the sample. This loss of quantum coherence can be attributed to the entanglement of the system states with the infinite set of states of the statistical environment. This prevailing idea of the decoherence is discussed in the literature under different aspects [24, 23]. In this work we focus on mesoscopic systems.

In the following, we will introduce some fundamental values that characterize the quantum coherence in mesoscopic samples. We will also give a brief review of the transport theory for low-dimensional systems and of the experimental techniques that have allowed to measure these values.

## 2.1 Characteristic lengths

The size of a conductor usually determines its transport behavior. For example, a sample shows an ohmic behavior, when its dimensions are much larger than certain characteristic lengths, such as (i) the Fermi wave length, (ii) the mean free path and (iii) the phase-coherence length. In a mesoscopic system, however, the dimensions are of the order of these characteristic lengths, so that one can still observe quantum coherence effects. We will discuss all the relevant length scales one by one.

### 2.1.1 Mean Free Path

The mean free path  $L_m$  is the distance covered by an electron before its initial momentum is destroyed. The associated relaxation time  $\tau$  is inversely proportional to the probability of scattering from a state with an initial momentum to another state with a different momentum. Thus, in metallic systems at low temperatures, where the transport is due to electrons close to the Fermi level, the mean free path is given by

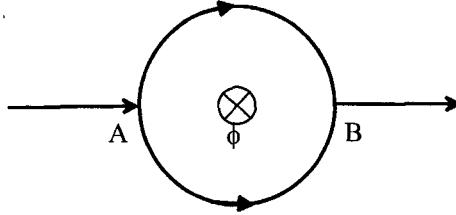
$$L_m = v_F \tau, \quad (2.2)$$

where  $v_F = \hbar k_F / m$  is the Fermi velocity to the Fermi wave vector  $k_F$ . The latter varies as a function of electron density  $n$ . In a  $d$  dimensional system it is proportional to  $k_F \propto n^{1/d}$ .

### 2.1.2 Fermi Wave Length

The length corresponding to the Fermi wave vector,  $\lambda_F = 2\pi/k_F$ , is much shorter than the mean free path in macroscopic metallic systems. The electrons with kinetic energy less than the Fermi energy have longer wave lengths, but at low temperatures they do not contribute to the dc transport so that the Fermi wave length represents the relevant length scale in this case. A comparison between the

Figure 2.1: The incoming electron beam is separated into two paths at point A of the metallic ring. In the full coherent case, the quantum interferences at B can be changed from constructive to destructive by varying the magnetic flux



sample dimensions and  $\lambda_F$  determines the effective dimensionality of the system. If all the three dimensions of the sample are much larger than  $\lambda_F$ , the system is truly three-dimensional. Quantum wells, quantum wires and quantum dots are obtained by reducing one or more of the edges of the sample to the order of  $\lambda_F$ .

### 2.1.3 Thermal Diffusion Length

A finite mean free path leads to a particular transport behavior in the presence of disorder [2]. On length scales longer than  $L_m$ , the system can then be considered as diffusive and the electronic propagation can be characterized by the diffusion constant  $D = v_F^2 \tau / d$ , where  $d$  stands for the dimensionality. In this regime, the energy of every Bloch state is broadened by approximately  $\hbar/\tau$ . The phase of the wavefunctions belonging to these eigenvalues has a definite correlation and the phase coherence of a particular state is not destroyed by random scatterers.

The characteristic length in this regime is given by

$$L_T = \sqrt{D\hbar/k_B T}, \quad (2.3)$$

$k_B$  being the Boltzmann constant. The quantity  $\hbar/k_B T$  is the time scale corresponding to the thermal broadening of the Fermi distribution, so that  $L_T$  can be considered as a length over which the coherence effects still persist when averaged over states near the Fermi energy within the thermal broadening.

### 2.1.4 Phase-Coherence Length

All the length scales above are introduced within the framework of the one-particle picture, where interactions, such as the electron-phonon or the Coulomb interaction, are neglected. The phase-coherence length characterizes a sample, taking into account also the inelastic scattering processes.

Fig. 2.1 shows a situation, in which a beam of electrons is split into two paths at the point A and is recombined at the point B. In the absence of additional

backscattering in the leads, the two paths are identical and the resulting interference at point B is constructive. The amplitude of the interference pattern will reduce in the presence of elastic or inelastic backscattering of the electrons by impurities, defects, phonons, etc. If the latter are thermally distributed they add a random phase to the scattered electrons, so that constructive interference at point B is destroyed. For scattering by static impurities one has a definite phase relation between the two paths. Since magnetic field gives rise to an additional phase factor by breaking the symmetry of the ring [25, 26], the interference pattern in this case can be changed from destructive to constructive just by applying an appropriate constant magnetic field through the ring. In the case of dynamic scatterers, such as phonons, the phase relation between the scattered waves varies randomly in time. A constant magnetic field will then only result in a random fluctuation of the interference amplitude, whose average over time goes to zero. The phase-coherence length  $L_\phi$  is defined as the distance over which the phase relations continue to persist.

The phase-coherence time  $\tau_\phi$  is the characteristic time attributed to  $L_\phi$ . In a naive first approach one could think that  $\tau_\phi$  is equal to the collision time. However, a simple argument shows that this is not necessarily true. In fact, a phonon, which interacts identically with both paths, would randomly change the phase of the electrons without affecting their phase difference. The simplest way to find a relation between  $L_\phi$  and  $\tau_\phi$  seems to be

$$L_\phi = v_F \tau_\phi. \quad (2.4)$$

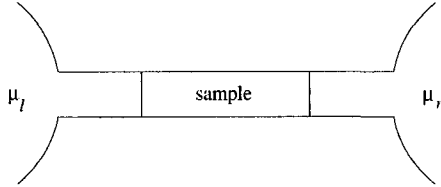
Definition 2.4 is, however, only acceptable, if the mean free path  $L_m$  is of the same order or shorter than  $L_\phi$ . In most metallic samples, however,  $L_m \ll L_\phi$  so that the trajectory of an electron during  $\tau_\phi$  is rather characterized by diffusion. In this case, the relation between  $L_\phi$  and  $\tau_\phi$  becomes

$$L_\phi^2 = D\tau_\phi. \quad (2.5)$$

## 2.2 Landauer Picture of Transport

Landauer [27] investigated electronic dc transport in a one-dimensional wire, dividing the whole system into two subsystems: (i) A sample connected by long ideal leads at both ends to (ii) two electron reservoirs with chemical potentials  $\mu_l$  (left reservoir) and  $\mu_r$  (right reservoir) near the Fermi energy of the quantum wire (Fig. 2.2). The two ideal reservoirs are statistically independent and absorb incident electrons regardless of their energy or phase. In this picture all the phase destroying and dissipative processes take place in the reservoirs and not

Figure 2.2: A sample connected to two reservoirs with chemical potentials  $\mu_l > \mu_r$ .



in the sample. It is important to note that within the framework of this model the reservoirs are by definition *infinite*, since otherwise the chemical potential of finite reservoirs would change with time in the presence of a direct current. Moreover, complete electronic dissipation is guaranteed only in infinite reservoirs. The Landauer formula relates the conductivity  $G$  to the transmission probability  $\hat{T}$  of the electrons in the sample. At zero temperature and if the contact resistance is neglected, it reads

$$G = \frac{2e^2}{h} \hat{T}. \quad (2.6)$$

Thus, in the linear response regime and at zero temperature, the current in the two-terminal device (Fig. 2.2) can be expressed as

$$I = \frac{2e}{h} \hat{T} \Delta\mu, \quad (2.7)$$

with  $\Delta\mu$  being the difference between the chemical potentials of the left and right reservoirs. The description can easily be extended to many-terminal devices. In fact, there is no qualitative difference between terminals so that they can be treated in an equal manner. Imagine a many-terminal device, where the terminal leads  $j$  are connected to different reservoirs with corresponding chemical potentials  $\mu_j$ . The current flowing through a specific terminal  $i$  is obtained by summing over all terminals

$$I_i = \frac{2e}{h} \sum_j [\hat{T}_{i \rightarrow j} \mu_i - \hat{T}_{j \rightarrow i} \mu_j], \quad (2.8)$$

where the arrows in the indices of the transmission coefficients indicate the direction of the electron transfer between two terminals  $i$  and  $j$ .

Assuming a Fermi distribution for the electrons, the description can be extended to non-zero temperatures. This assumption is, however, strictly correct only at equilibrium and its extension to the dc transport problem must be considered as a rough approximation of the true electronic distribution functions. At a given temperature  $T$  the energy distribution of the electrons in a reservoir with the chemical potential  $\mu_i$  is then determined by the Fermi function of the latter

$$f_i(E, T) = \frac{1}{\exp(E - \mu_i/k_B T) + 1}. \quad (2.9)$$

In quasi-one-dimensional (quasi-1D) quantum wires, the transport takes place in several channels or propagating states that in general possess different transmission probabilities. Including the back- and forward current at any point in the two-terminal device, one obtains for the net current through a single channel

$$i(E) = \frac{2e}{h} \hat{T}(E) [f_l(E, T) - f_r(E, T)], \quad (2.10)$$

where  $f_l(E, T)$  ( $f_r(E, T)$ ) represent the electronic distribution in the left (right) reservoir, and where we have assumed that the transmission does not depend on the direction. This is always true for time-independent elastic scatterers in the sample. The assumption of the left-right symmetry is not valid for scattering by general time-dependent potentials  $V(t)$ . In Ref. [28], it is shown that a mesoscopic pump can be constructed using the inequality between the back- and forward scattering. The total current results from the sum of  $i(E)$  over all channels. In analogy to Eq. 2.8, for multi-terminal devices, the current in the channels can be written as

$$i_j(E) = \frac{2e}{h} \sum_k [\hat{T}_{j \rightarrow k} f_j(E, T) - \hat{T}_{k \rightarrow j} f_k(E, T)]. \quad (2.11)$$

In the absence of time-dependent scattering potentials, the transmission coefficients satisfy the sum rule

$$\sum_k \hat{T}_{k \rightarrow j} = \sum_k \hat{T}_{j \rightarrow k} \quad (2.12)$$

so that Eq. 2.11 can be expressed in the form

$$i_j(E) = \frac{2e}{h} \sum_k \hat{T}_{kj} [f_j(E, T) - f_k(E, T)], \quad (2.13)$$

where we have disposed of the notation  $\hat{T}_{kj} = \hat{T}_{k \rightarrow j}$ .

### 2.2.1 Aspects of Landauer-Büttiker Approach

There are some points in this formalism that need more clarification. From the energetic point of view it still remains the question where the Joule heat is dissipated. If the scatterers in the sample are static without any internal degrees of freedom, they cannot dissipate energy. Energy dissipation can only occur through inelastic processes like phonon emission. At first glance this does not seem like a very significant problem for the electronic transport, which is, according to the Landauer formula, essentially determined by the momentum relaxation of the electrons and not by their energy relaxation. Its importance, however, becomes more obvious, when one tries to describe the transition from the fully coherent to the ohmic regime.

Büttiker has accounted for dissipation in the sample using a multi-terminal approach by introducing phase-randomizing “fictitious voltage probes” [10]. The latter are connected to electron reservoirs, whose chemical potential is determined such that the voltage probe conserves the current and introduces a loss of phase coherence and a change of electron energy. In this picture the net current, flowing from the first to the second terminal, is divided into two components: (i) the coherently transmitted part of electrons which pass through the sample without entering any voltage probe, and (ii) the incoherent fraction of electrons, which have entered in one or more voltage probes, having their phase randomized and energy changed before reaching the second terminal. The flow of the current between the terminals is assumed to be fully coherent. The physical idea behind this phenomenological approach is to simulate the phase breaking processes and energy changes by introducing thermalization within the reservoirs attached to the virtual voltage probes. It can be shown that this method is equivalent to introducing a finite life time to particles in a fully coherent system [29]. In this approach, the Joule heat is generated by changes of the local electron energy. In a microscopic picture, the excess of energy would eventually be dissipated to the lattice.

Another crucial point in the Landauer-Büttiker formalism is the role of the Pauli exclusion principle. The question whether Eq. 2.13 should be modified to

$$i_j(E) = \frac{2e}{h} \sum_k [\hat{T}_{kj} f_j(E, T)(1 - f_k(E, T)) - \hat{T}_{jk} f_k(E, T)(1 - f_j(E, T))] \quad (2.14)$$

or not (see for example [30]) has initially attracted little scientific interest, since this modification has no effect on the description of the electron transport in the absence of inelastic scattering processes. In fact, the terms containing  $f_j(E, T)f_k(E, T)$  cancel in Eq. 2.14 and there is finally no difference between the right-hand sides of the equations 2.11 and 2.14. But the situation changes, when the sum rule Eq. 2.12 is not satisfied. In a fully coherent system, any occupied scattering state will contribute to the current, and Pauli blocking cannot occur. This is due to the fact that the time evolution of the coherent system is determined by a unitary time-evolution operator. The situation changes, however, for the non-coherent transport, in which real electronic transitions take place due to inelastic scattering processes.

The effect of the exclusion principle on the non-coherent electronic transport is more complicated than described by Eq. 2.14. In general, the current is comprised of both, a coherent and a non-coherent component. While, according to the above argument, no extra factor is needed for describing the Pauli exclusion in the coherent component of the current, it is also not correct to account for its

effect on the non-coherent part just by simply inserting  $(1 - f)$  factors as is done in Eq. 2.14. A better understanding of the role of the Pauli exclusion principle for the electronic transport requires a detailed microscopic theory including the role of the contacts and the reservoirs.

The two points, discussed above, have the same origin. Both are closely related with the interaction between the sample system and its environment. In chapter 3, we will discuss the effects of contacts and reservoirs in particular on the dc transport properties of mesoscopic systems.

## 2.3 Experimental Techniques

As previously mentioned, different length scales determine the characteristics of a system. The phase-coherence length is certainly the scale that gives the most interesting information about the behavior of the sample, especially at low temperatures. It has therefore been the object of numerous experimental investigations during the past decade. In this section we describe two experimental methods, which are generally employed to measure  $L_\phi$ .

### 2.3.1 Aharonov-Bohm Effect

At very low temperatures the resistance of small loops Fig. 2.1 shows periodic oscillations as a function of the magnetic field. This phenomenon, briefly discussed in subsection 2.1.4, is known as the Aharonov-Bohm (AB) effect. The size of the AB oscillations scales with two characteristic lengths  $L_\phi$  and  $L_T$ . When both length scales are much longer than the circumference of the ring, the root mean square of AB oscillations in the conductance  $\Delta g_{AB}$  approaches its universal value  $2e^2/h$ . The amplitude of these oscillations is proportional to the fraction of phase coherent carriers. Taking into account that the amplitude reduces through energy averaging, the AB scaling equation reads [31]

$$\Delta g_{AB} = \alpha \frac{e^2}{h} \frac{\pi L_T}{L} \exp(-L/L_\phi), \quad (2.15)$$

where  $\alpha$  is a number of the order of 1 that accounts for the sample geometry. This scaling behavior is, however, only expected for the case  $L \gg L_T$ , since the factor  $L_T/L$  is due to the energy averaging. In the opposite limit,  $L \ll L_T$ , the energy averaging does not come into play and the factor  $L_T/L$  is replaced by 1.

Other authors [32] have numerically calculated the scaling of AB oscillations for a different geometry and added some corrections to Eq. 2.15. In any case, the phase-coherence length can be obtained by means of the AB scaling equation, if the numerical factor  $\alpha$  is known. In practice one measures the AB oscillations for

a series of samples with the same geometry but of the different lengths  $L$  (see e.g. [33] and the references therein). The prefactor  $\alpha$  being approximately the same for these samples, one can estimate it by fitting the length dependence of  $\Delta g_{AB}$  at each temperature.  $L_\phi$  can then be obtained by means of the Eq. 2.15.

### 2.3.2 Weak Localization Regime

When applying the Landauer formula to a disordered single-mode conductor, one finds that the resistance  $\rho(L)$  increases exponentially with the sample length [1]. Thouless stated that even a multi-moded quasi-1D conductor shows this non-linear dependence, if its zero temperature resistance exceeds a critical value of the order  $h/2e^2$  [3]. In other words, if the sample is longer than a characteristic length, known as localization length  $L_{loc}$ , its resistance should increase exponentially with the length. However, this non-linear behavior can only be seen if the phase-coherence length is at least of the same order as  $L_{loc}$ . In this case, the conductor is said to be in the strong localization regime.

If  $L_\phi \ll L_{loc}$ , the conductor is said to be in the weak localization regime. Expanding the resistance in a Taylor series in this regime one finds [4]

$$\hat{\rho}(L) \approx \left[ \frac{L}{L_{loc}} + \left( \frac{L}{L_{loc}} \right)^2 \right], \quad (2.16)$$

where  $\hat{\rho}(L)$  is expressed in units of  $h/2e^2$ , i.e.  $\rho(L) = \hat{\rho}(L)h/2e^2$ . The first term on the right hand side is the classical term, while the second term represents a quantum correction  $\Delta\rho$  to the resistance. This correction arises from the constructive interference of time-reversed backscattered electron paths. The phase-coherence between the pairs of time-reversed trajectories, which start and end in the same mode, doubles the probability of reflection and so decreases the conductance.

In a quasi-1D sample with a width  $W$  shorter than  $L_\phi$ , the amplitude of this quantum correction to the conductance is [34, 35]

$$\delta G = -\frac{2e^2}{h} \frac{\sqrt{D}}{L} \left[ \tau_\phi^{\frac{1}{2}} + \left( \frac{1}{\tau_\phi} + \frac{1}{\tau} \right)^{-\frac{1}{2}} \right] \quad (2.17)$$

and for quasi-two-dimensional samples one finds

$$\delta G = -\frac{e^2}{\pi h} \ln \left[ \frac{\tau_\phi}{\tau} + 1 \right]. \quad (2.18)$$

It is thus sufficient to measure  $\delta G$  in order to determine  $\tau_\phi$ . The simplest way to do this is to apply a magnetic field perpendicular to the sample. The time-reversal symmetry can effectively be broken by sufficiently large fields, when the magnetic flux enclosed by a possible time-reversed pair of a given dimension is large enough to change the AB phase by  $\approx \pi$ .



## Chapter 3

# Dissipation in Electronically Open Systems

---

Multiple elastic scattering of electrons in mesoscopic systems at sample boundaries, potential barriers or impurities is at the origin of quantum interference effects which can be observed in the dc transport properties. The most prominent examples are Aharonov-Bohm oscillations or universal conductance fluctuations which have been both widely studied in the literature, as well experimentally as theoretically [36, 37, 38]. Quantum interference effects rely on the phase coherence of the electronic wave functions. It is thus important to understand the physical processes limiting the phase coherence in mesoscopic systems. Despite considerable progress in the general understanding of coherence phenomena in mesoscopic systems, a satisfactory theoretical description of the mechanisms underlying the loss of phase coherence is still missing. At high temperatures, dissipation is undoubtedly dominated by inelastic electron-phonon scattering, and interference effects are completely suppressed even in small samples. In the absence of elastic scattering, fully coherent propagating electronic states are expected for translational invariant systems at zero temperature [39]. Recent experiments on weakly disordered quasi-2D systems indicate that in the limit of low temperatures the phase-coherence time of the electron states does not become infinite but rather saturates.

Universal quantization of the dc conductance in units of  $2e^2/h$  is a characteristic feature of quantum wires. Experimentally, it has been observed in different situations, and a well elaborated theoretical explanation for this phenomenon has already found a wide acceptance in the scientific community.

Recently, several groups have, however, reported that the dc conductance in perfect mesoscopic quantum wires shows in fact nonuniversal conductance steps  $(2e^2/h)\nu$  with  $\nu < 1$ . This behavior could not be explained within the framework of known models with either interacting or non-interacting electrons in the sample.

In the following we show that these surprising features are possibly related and may be explained in quite similar term. Our argument is based on the *openness* of the electronic system, which implies that electrons in “occupied” states in the sample can always diffuse further away.

### 3.1 Phase-Coherence Time at Low Temperatures

Several recent experiments on quasi-1D Au wires [15], GaAs/Al<sub>x</sub>Ga<sub>1-x</sub>As heterostructures [40], as well as on GaAs/Al<sub>x</sub>Ga<sub>1-x</sub>As ballistic quantum dots [41] and normal-metal/superconductor samples [42] have shown a saturation of the phase-coherence time  $\tau_\phi$  at low temperatures rather than the expected increase versus infinity.

Starting from the assumption that electron-phonon scattering can be neglected at low temperatures, Mohanty *et al.* [43] gave a tentative explanation in terms of electron-electron scattering, where electrons contributing to the transport are scattered by the zero-point fluctuations of the electromagnetic environment accompanying the fluctuations of the N-particle density. In this picture, the zero-point fluctuations dominate at low temperatures and give rise to phase-destructive scattering even in the limit of zero temperature. Other authors have attempted to explain this behavior in terms of electron-electron interactions within the sample [40, 44, 45]. These explanations are, however, not completely satisfactory. A consistent approach taking into account the entanglement of the electronic states would require a description of transport properties in terms of the correlated collective motion of *all* electrons instead of using an effective one-electron picture, where the effect of the electrons in the background is reduced to dephasing the one-particle states. In Ref. [46] the low-temperature saturation of  $\tau_\phi$  is proposed to be due to the external electromagnetic noise.

Here we propose an alternative explanation of low-temperature decoherence. We start from the idea that dephasing is caused by the interaction between the sample and its environment even at zero temperature. This becomes possible if we explicitly take into account the fact that the system is open, which is particularly appropriate under the here-considered dc conditions, where the system is linked to dissipating reservoirs. While the authors of Ref. [43] account for the dissipative phase-destroying phonon-absorption processes at finite temperatures, they assume that under the experimental conditions, i.e., at low electric fields and low temperatures, electron scattering involving phonon-emission processes is suppressed by the Pauli exclusion principle. This assumption is, however, not strictly correct. The Pauli exclusion principle is only valid in *closed* systems and cannot be applied to *open* systems, i.e. systems connected to reservoirs, where the number of

electron states per (infinitesimal) energy interval is infinite. In other words, while at low temperature and low fields Pauli blocking suppresses transitions into states below the Fermi energy in closed systems, it is also obvious that this suppression becomes at least less important when the system is gradually opened, so that supernumerary electrons can escape the sample region. This immediately shows that, contrary to the arguments in the literature, phonon-emission processes may quite well be important and should at least be reconsidered. Our present problem is closely related to the question already raised by R. Landauer[30], mentioned in subsection 2.2.1, whether the Pauli exclusion principle has to be considered or not for electrons entering the external reservoirs under dc conditions. In the following we will show that the experimental results can in fact be explained by accounting for phonon-emission contributions.

### 3.1.1 Phase-Coherence Time in Presence of Electron-Phonon Scattering Processes

Starting from the Landauer picture for dc transport, we consider a two-terminal device and assume weak electron-phonon interaction. Electron scattering by phonons can then be described on the level of one-phonon emission or one-phonon absorption processes. Both the electron and the phonon subsystems are open. The thermal coupling of the phonons to the environment leads to a finite phonon lifetime  $\tau_{phon}$ . The electrons are coupled to two statistically independent reservoirs with chemical potentials near the Fermi energy  $E_F$  of the closed electron system. Even for vanishing electron-phonon interactions, this coupling to the reservoirs implies a finite lifetime  $\tau_{res}$  for electrons in the mesoscopic subsystem that we consider. This case has been treated by Lang [47] and Datta *et al.* [48] experimentally as well as theoretically for very small systems, e.g. few-atom systems in a scanning tunneling microscope. The interaction between electrons and reservoirs decreases with the sample size. The thermal coupling with the environment is controlled by the rather strong vibrational interaction between the mesoscopic subsystem and the substrate. For sufficiently large samples, or small electronic escape rate, we may therefore assume  $\tau_{phon} \ll \tau_{res}$ . Thus prepared, we can now introduce the effects of electron-phonon coupling on the lifetime of electrons. In order to discuss properly transitions between one-electron states with initial energy  $E_i$  and final energy  $E_f$ , we have to ensure that the interaction time  $\tau$  is sufficiently large for the dominant one-phonon transitions, i.e.,

$$\Delta E \tau \geq 2\pi \text{ with } \Delta E = E_i - E_f. \quad (3.1)$$

The interaction time is limited by the lifetime of the phonons, i.e. we have

$$1/\tau > 1/\tau_{phon} \gg 1/\tau_{res}. \quad (3.2)$$

The effective lifetime  $\tau_{eff}$  of an electron near the Fermi energy is then given by

$$1/\tau_{eff} = 1/\tau_{res} + 1/\tau_e + 1/\tau_a \quad (3.3)$$

where  $\tau_e$  ( $\tau_a$ ) corresponds to one-phonon emission (absorption) processes. We use Fermi's golden rule, to calculate the phase-coherence time  $\tau_\phi$  in presence of electron-phonon interactions. The effective electron-phonon coupling can be characterized by

$$\frac{1}{\tau_o} = \int_0^{\omega_D} M_{el-ph}(\omega)g(\omega)d\omega, \quad (3.4)$$

where  $M_{el-ph}$  represents the coupling matrix element. For weak coupling, i.e.  $1/\tau_o < 1/\tau_{phon}$ , the phonons participating in successive scattering processes become statistically independent, and we get

$$\frac{1}{\tau_\phi(E)} = \int_0^{\omega_D} M_{el-ph} [1 - \alpha f(E - \omega)] g(\omega) d\omega + \int_0^{\omega_D} \frac{M_{el-ph}}{e^{\frac{\hbar\omega}{k_B T}} - 1} [1 - \alpha f(E + \omega)] g(\omega) d\omega. \quad (3.5)$$

Here  $g(\omega)$  is the phonon density of states and  $f(E)$  is the Fermi distribution function. The reduction factor  $\alpha \in [0, 1]$  accounts for the loss of electrons into the reservoirs,  $\alpha = 1$  corresponds to complete Pauli blocking in a closed system, for  $\alpha = 0$  we have no Pauli blocking at all. In the following we chose  $E = E_F$  for the electron energy. Note that we use the elementary form in Eq. 3.5 rather than the description in terms of the Éliashberg coupling function[49], since the latter already includes the Pauli blocking.

For the two-dimensional case we have  $g(\omega) = 2\pi\omega/c$ , with  $c$  being the group velocity of the longitudinal phonons. With the substitutions  $\Theta_D = \hbar\omega_D/k_B$ , and  $x = \frac{\hbar\omega}{k_B T}$ , Eq. 3.5 reads

$$\frac{1}{\tau_\phi} = T^2 \int_0^{\frac{\Theta_D}{T}} \tilde{M}_{el-ph}(xT) x \frac{(1 - \alpha)e^{2x} + (1 + \alpha)e^x - \alpha}{e^{2x} - 1} dx. \quad (3.6)$$

Here, the modified matrix element  $\tilde{M}_{el-ph}(xT)$  can be approximated as

$$\tilde{M}_{el-ph}(xT) \simeq \eta x T. \quad (3.7)$$

Eq. 3.6 is valid under the above mentioned conditions

$$1/\tau > 1/\tau_{phon} > 1/\tau_o \gg 1/\tau_{res}. \quad (3.8)$$

From Equations. 3.5 and 3.6 it follows that the electron-phonon emission term leads to finite phase-coherence time for  $\alpha < 1$  even at  $T = 0$ .

The dephasing rate in Eq. 3.6 is defined by the coupling factor  $\eta$  depending on the specific material, and by the reduction factor  $\alpha$  which describes the coupling

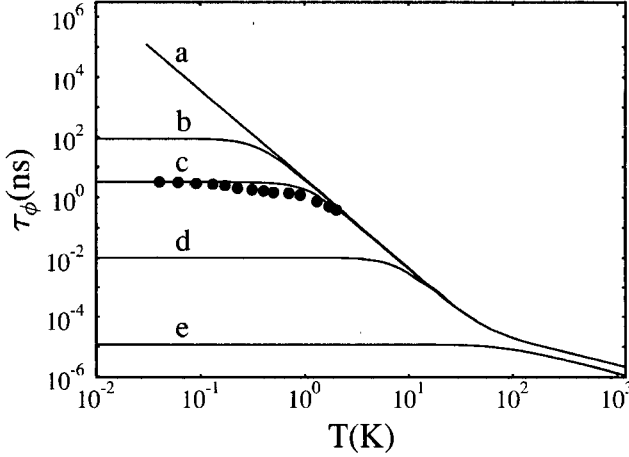


Figure 3.1: Temperature dependence of the phase-coherence time. The points represent the experimental results of Ref. [43]. Curves  $a, \dots, e$  are calculated from Eq. 3.5 for  $\eta = 0.058 \text{ s}^{-1} \text{ K}^{-3}$  and different  $\alpha$  values, a)  $\alpha = 1$ ; b)  $\alpha = 0.9999999$ ; c)  $\alpha = 0.9999971$ ; d)  $\alpha = 0.999$ ; e)  $\alpha = 0$ .

to the reservoirs and thus depends on the sample configuration. We note that the high-temperature behavior is controlled by  $\eta$  alone, whereas the low-temperature behavior is determined by  $\alpha$ .

In Fig. 3.1 we show the temperature-dependence of the dephasing time for  $\eta = 0.058 \text{ s}^{-1} \text{ K}^{-3}$  and different  $\alpha$  parameters. The coupling parameter was chosen to fit the experimental results of Mohanty *et al.* [43] for a Au quantum wire, which are also represented. The curves were obtained with  $\Theta_D = 170 \text{ K}$  which corresponds to the case of Au.

An excellent fit of the experimental points from Ref. [43] is obtained with  $\alpha = 0.9999971$  (curve  $c$  in Fig. 3.1). Comparison with the case of complete Pauli blocking ( $\alpha = 1$ ) shows that the experimental results can be explained assuming a finite but extremely small probability rate for the electrons to escape the sample region.

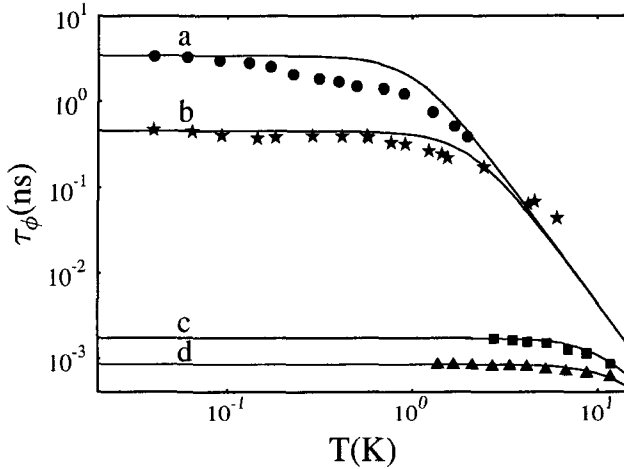


Figure 3.2: Temperature dependence of the phase-coherence time for Au (upper two curves, corresponding to the samples Au-1 and Au-5 in Ref. [15]; the uppermost curve is identical with the experimental curve in Fig. 3.1) and for the evaporated Pd-Au samples of Ref. [50] (lower two curves). The theoretical fits given by the full lines correspond to  $\Theta_D = 170\text{K}$  and a)  $\eta = 0.058\text{s}^{-1}\text{K}^{-3}$ ,  $\alpha = 0.9999971$ ; b)  $\eta = 0.058\text{s}^{-1}\text{K}^{-3}$ ,  $\alpha = 0.9999978$ ; c)  $\eta = 0.09\text{s}^{-1}\text{K}^{-3}$ ,  $\alpha = 0.99595$ ; d)  $\eta = 0.09\text{s}^{-1}\text{K}^{-3}$ ,  $\alpha = 0.9916$ .

### 3.1.2 Discussion and Suggestions for Further Investigations

From our theoretical analysis it follows immediately that the high-temperature behavior should be characteristic for the chosen material, whereas the low-temperature behavior should depend solely on the sample geometry and the contact configuration (see also curves *b*, *c* and *d* in Fig. 3.1). This is indeed confirmed by the existing experimental results (see Figs. 2 and 4 in Ref. [15]), which can also be described within our approach. As an example, we present further fits for Au [15] and for Pd-Au [50] in Fig. 3.2.

To check the consistency of our interpretation, we estimate the fraction  $p$  of electrons leaving the sample within the time interval  $\tau_o = \tau_\phi(\alpha = 0, T = 0)$ . Here,  $\tau_o$  measures the scattering time due to phonon emission only in the absence of any Pauli blocking. We obtain  $p = \sqrt{D\tau_o}/d$ , where  $d$  is the distance between the two contacts and  $D$  is the diffusion constant. The fraction  $p$  represents an upper

estimate of the free states below  $E_F$  which can be reached by electrons at  $E_F$  after phonon emission. In fact, additional scattering e.g. at the contacts and at the sample boundaries will lower the escape rate of the electrons in real samples with respect to the ideal value of  $D/d^2$ . Moreover, the above estimate does not account for the fact that, in addition to the phonon-emission path, states below  $E_F$  are also filled from the reservoirs. Both concurring paths are statistically independent and have to be treated on an equal basis. We thus expect

$$p > 1 - \alpha. \quad (3.9)$$

The validity of this relation can be checked if the diffusion constant  $D$  is known. We have found that it is satisfied for the Au samples of Ref. [15].

The coupling of electrons within the sample to the reservoirs depends on the sample size, on the contact geometry as well as on the presence of disorder or barriers. The correctness of the presented ideas could be experimentally verified by introducing for example variable barriers in the contact regions. According to our description, it should then be possible to systematically change the saturation value of the phase-coherence time at low temperatures by varying the barrier heights. Such a behavior is not expected within the dephasing models based on electron-electron scattering. A distinction between our picture of decoherence and the electron-electron based dephasing mechanism is thus possible.

## 3.2 Nonuniversal Conductance Steps

Though the universal conductance quantization in one-dimensional (1D) electronic systems was predicted long before, the first successful experiments, performed on ballistic point contacts defined in a two-dimensional electron gas of a GaAs-AlGaAs heterostructure [51], date late eighties. While these earlier experiments were performed at very low temperatures ( $T < 0.6K$ ), quantization was found more recently even in metallic break junctions at room temperature [52]. Universal conductance steps require the absence of electron backscattering within the sample. This explains why the direct confirmation of the quantization in quantum wires has not been possible for a long time. Elastic or inelastic backscattering can, however, be suppressed by exposing a 2D electron gas in a quantum wire to a perpendicular magnetic field. In this way the quantization can be recovered and leads to integer quantum Hall plateaus [53].

Only recently, Yacoby *et al.* [16] have succeeded to produce quantum wires as long as  $1 - 10\mu m$  of extreme quality. Quite surprisingly, the conductance steps found for these samples have heights  $(2e^2/h)\nu$ , with  $\nu = 0.8 \dots 0.9$  instead

of  $\nu = 1$ . In the meantime, these results have been confirmed by other groups [54, 55].

As was already discussed in Ref. [16], the nonuniversal step height can neither be explained by elastic impurity scattering nor by electron-electron interactions. Nevertheless, it is obvious that any decrease of the conductance with respect to its universal value must be due to either some backscattering mechanism or to a reduction of the number of non-equilibrium electrons participating in the transport at given bias. Most recently, Alekseev et al.[56] have attempted to explain the experimental results using the first type of argument. They argue that electrons exiting the 1D channels in the wire are partly scattered back at the contacts. In their picture, the scattering potential is caused by the Friedel oscillations of the charge density in the 2D gas behind the contacts. The experimentally observed increase of the step heights at larger bias or temperature is then explained by the reduced scattering probability in both cases. However, this approach, while interesting in itself, is not completely satisfactory. In particular, one should expect length-dependent Fabry-Pérot type oscillations of the conductance due to multiple scattering of electrons between the contacts instead of the observed well-defined conductance plateaus. We also believe that the existence of coherent scattering of electrons from the 2D electron gas behind the contacts back into the wire is questionable, since the 2D sections are in close thermal contact with the substrate. This implies that dissipative processes due to inelastic electron-phonon scattering should already be important in the region of the Friedel oscillations near the contacts.

In the following we employ the second type of argument. In contrast to Ref. [56] we will restrict our discussion to the linear response regime at small bias, and we will only consider the zero-temperature case. Our approach is based on the same argument as in the previous section. In *open* dc systems connected to electron reservoirs, non-equilibrium electrons coupled to states with lower energies by electron-phonon interaction can descend into these states even at zero temperature. The relevance of these transitions in open systems can be inferred from the observation that, without such processes, thermalization of non-equilibrium electrons entering an electron reservoir with a given chemical potential would be impossible in the low-temperature limit. Accepting this relaxation mechanism in the reservoirs, it is then quite natural to allow for these transitions also in the sample region. The resulting situation can be described within the Landauer picture of dc transport and assuming partial Pauli blocking in the reservoirs.

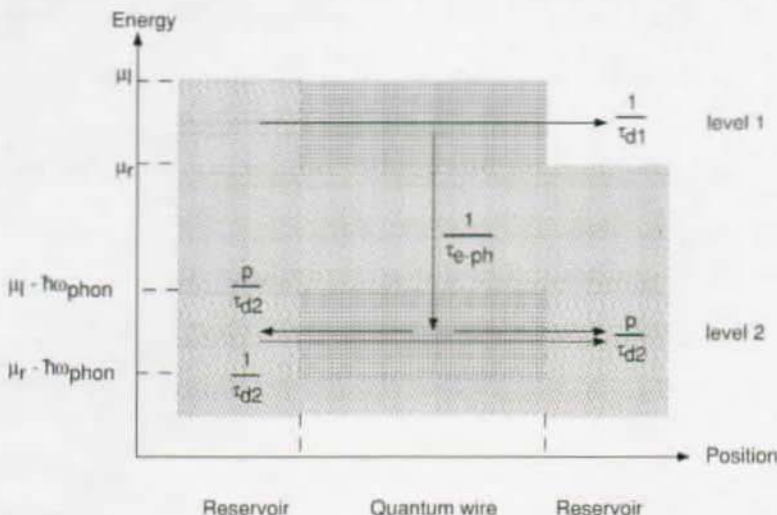


Figure 3.3: Quantum wire connected to external electron reservoirs. The electronic transitions considered in the rate equations Eqs. 3.11 and 3.12 are indicated by the arrows.

### 3.2.1 Model Description

We consider a mesoscopic wire connected to electron reservoirs at both ends. A direct current through the wire is maintained by keeping the two reservoirs at slightly different chemical potentials  $\mu_l$  and  $\mu_r$ . To be specific, we consider the case  $\mu_l > E_F > \mu_r$  (see Fig. 3.3), where  $E_F$  is the Fermi energy of the wire at equilibrium. We assume the wire and the contact regions to be free of elastic scattering centers or potential barriers.

Due to the lateral confinement of the electron gas in the quantum wire, the electronic states of the wire are split into 1D subbands. In the absence of elastic or inelastic scattering within the wire, the conductance is  $G = (2e^2/h) N(E_F)$ , where  $N(E_F)$  is the number of subbands crossing the Fermi-level. In the following we presume negligible interband electron-phonon coupling, but we allow for intraband coupling. Then, the current through the wire can be written as

$$J(E_F) = \sum_{s=1}^N j(E_F - \varepsilon_s), \quad (3.10)$$

where the sum runs over all subbands crossing the Fermi level,  $\varepsilon_s$  denotes the lower band edge of subband  $s$ . The contributions  $j(E)$  being independent of the

subband index  $s$ , it is sufficient to discuss the situation for a single subband  $t$  with the bottom energy  $\varepsilon_t \leq E_F$ . For simplicity, we assume a single transition energy  $\hbar\omega_{phon}$  for phonon emission processes, which may represent an optical phonon energy or the Debye frequency. The coupling between electron states separated by  $\hbar\omega_{phon}$  is given by the transition rate  $1/\tau_{e-ph}$ . This allows us to describe the situation within the sample by an effective two-level system, where the upper level 1 accounts for the ensemble of states in the interval  $\mu_r < \varepsilon < \mu_l$ , and the lower level 2 represents the ensemble of states in the interval  $\mu_r - \hbar\omega_{phon} < \varepsilon < \mu_l - \hbar\omega_{phon}$  (see Fig. 3.3).

### 3.2.2 Rate Equations

In the following we derive the rate equations that determine the occupation of both levels at low temperatures with  $kT \ll \hbar\omega_{phon}$ . Under the above assumptions, only states propagating from left to right can be occupied in level 1, whereas electrons in level 2 travel in both directions. Nevertheless, as long as we assume equal scattering probability from level 1 into both propagation directions in level 2, the occupation probability is the same for left-right and right-left traveling states, and we only need to calculate one of both.

In the absence of phonon-emission processes, we have the standard situation: Electrons are injected from the left into level 1, travel through the wire, before being reabsorbed by the right reservoir; electrons in level 2 do not contribute to the total current, regardless of the made assumptions about the partial currents from left to right or from right to left. The conductance is quantized in units of  $2e^2/h$ .

The physics becomes much more involved, when we allow for inelastic scattering due to phonon emission. Electrons in subbands  $t$  with energies  $E \simeq E_F > \varepsilon_t + \hbar\omega_{phon}$ , which have entered the sample from the left reservoir may then be scattered into level 2. The ensemble of electrons in level 2 traveling from left to right can thus be reached from level 1 as well as from the left reservoir. Both sources being statistically independent, we have to account for Pauli blocking effects, i.e., we have to ensure that electrons attempting to enter level 2 from the left reservoir, are only allowed to occupy states which are not yet occupied by electrons which have entered through level 1<sup>1</sup>. Similarly, electrons from level 1 can only enter states in level 2 which are not yet occupied by statistically independent electrons. For  $E_F - \varepsilon_t > \hbar\omega_{phon}$ , the stationary occupations  $n_1$  and  $n_2$  in

<sup>1</sup>Pauli blocking does not concern coherent electrons, since the coherent dynamics of electrons entering from one source is described by a unitary evolution operator keeping the electron states orthogonal at each time. Therefore, as long as coherence is guaranteed, multiple occupation of electron states is impossible, and Pauli exclusion does not come into play [30].

levels 1 and 2 by electrons traveling from left to right obey the rate equations

$$\frac{1}{\tau_{d1}} = 2 \frac{n_1}{\tau_{e-ph}} (1 - n_2 + \delta) + \frac{n_1}{\tau_{d1}} \quad (3.11)$$

$$\frac{1 - n_{2,1}}{\tau_{d2}} = - \frac{n_1}{\tau_{e-ph}} (1 - n_2 + \delta) + p \frac{n_2}{\tau_{d2}}. \quad (3.12)$$

Here we have assumed that electrons in level 1 are scattered with equal probability into both propagation directions in level 2. This leads to the factor 2 in Eq. 3.11. The electron-phonon interaction is given by the scattering rate  $1/\tau_{e-ph}$ . The transit times per unit length,  $\tau_{d1}$  and  $\tau_{d2}$ , are obtained from the reciprocal group velocities in the considered subband at energies  $E_F$  and  $E_F - \hbar\omega_{phon}$ , respectively. The partial occupation  $n_{2,1}$  describes the fraction of electrons which have entered level 2 from level 1, and  $\delta$  represents the related fraction of electrons in level 2, which again have entered through level 1, but now within a time interval given by the phonon-coherence time  $\tau_{phon}$ . The electrons described by the parameter  $\delta$  are still coherent with electrons entering from level 1, and therefore they do not contribute to the Pauli blocking of transitions from level 1 to level 2. In a semi-classical picture we obtain

$$\delta \approx n_{2,1} \frac{\tau_{phon}}{\tau_{d1}}. \quad (3.13)$$

In the following we will assume  $\tau_{phon} \simeq \tau_{e-ph}$ <sup>2</sup>. The factor  $p$  in Eq. 3.12 gives the probability  $0 < p < 1$  to enter the reservoirs from level 2. The absence of any Pauli blocking in the reservoirs is described by  $p = 1$ , full Pauli blocking corresponding to closed systems is obtained with  $p = 0$ . Following our above arguments, electrons occupying reservoir states interacting with the sample region may always diffuse further away into empty states, i.e., the reservoirs should be regarded as leaking rather than as closed systems. We thus expect a non-vanishing probability  $p$  for the electrons in level 2 to enter the left and right reservoirs.

### 3.2.3 Energy Dependence of Level Occupation

We emphasize that the rate equations 3.11 and 3.12 can of course not describe any effects due to the coherent evolution of the electronic states within the time

<sup>2</sup>With this assumption the phonons are still well defined, but coherent multiple-phonon processes leading to polaron effects become negligible. We will see later (see Eq. 3.17), that formally this assumption becomes irrelevant for our description in the limit of sufficiently large electron-phonon coupling. For reasons of consistency, however, the condition  $\tau_{phon} \leq \tau_{e-ph}$  remains necessary, since otherwise we would have to describe the effects of the electron-phonon interaction on the *coherent* evolution of the electron states, which is beyond the possibilities of the present approach based on rate equations.

interval  $0 < t < \tau_{phon}$ . In the following we therefore restrict ourselves to the discussion of the results in the limit  $\delta \rightarrow 0$ , where coherence effects become unimportant. The introduction of the parameter  $\delta$  in Eqs. 3.11 and 3.12 is, however, necessary, in order to find the solution with the correct limiting behavior, as will be seen below.

Under our above assumption of equal inelastic back- and forward scattering probabilities, the forward and backward current contributions from electrons in level 2 cancel, and the contribution to the current from a single subband becomes

$$j = (2e^2/h) n_1. \quad (3.14)$$

We thus have to calculate the occupation  $n_1$ . The system of the three equations 3.11, 3.12 and 3.13 is, however, still underdetermined, since it contains four unknowns  $n_1$ ,  $n_2$ ,  $n_{2,1}$  and  $\delta$ . We therefore have to look for a supplementary condition, which defines the relative importance of the two independent entries into level 2. For this purpose we introduce the partial occupation  $n_{2,res}$  which represents the fraction of electrons in level 2 having entered through the left reservoir. It obeys the sum rule

$$n_2 = n_{2,1} + n_{2,res}. \quad (3.15)$$

The ratio  $n_{2,1}/n_{2,res}$  is determined by the ratio between the respective rates  $1/\tau_{e-ph}$  and  $1/\tau_{d2}$ , i.e.

$$\frac{n_{2,1}}{n_{2,res}} = \frac{\tau_{d2}}{\tau_{e-ph}}. \quad (3.16)$$

Equations 3.11, 3.12, 3.13, 3.15, and 3.16 define the five unknowns  $n_1$ ,  $n_2$ ,  $n_{2,1}$ ,  $n_{2,res}$ , and  $\delta$ . These equations are readily solved for any set of parameters. In the limit of large electron-phonon coupling with  $\tau_{e-ph}/\tau_{d1} \rightarrow 0$ <sup>3</sup> and assuming parabolic dispersion for the 1D subbands we obtain

$$n_1(\tilde{\varepsilon}) = \begin{cases} 1 & \text{for } \tilde{\varepsilon} = \frac{E_F - \varepsilon_t}{\hbar\omega_{phon}} \text{ and } 0 < \tilde{\varepsilon} < 1 \\ 1 - 2p \frac{\tau_{d1}}{\tau_{d2}} = 1 - 2p \sqrt{\frac{\tilde{\varepsilon} - 1}{\tilde{\varepsilon}}} & \tilde{\varepsilon} > 1. \end{cases} \quad (3.17)$$

The corresponding solutions for the other parameters are  $\delta = 0$ ,  $n_{2,1} = n_2 = 1$ , and  $n_{2,res} = 0$ . From Eq. 3.17 we obtain for the saturation value

$$n_1(\infty) = 1 - 2p, \quad (3.18)$$

which together with Eq. 3.14 leads to the conductance step height  $\nu = 1 - 2p$ . The resulting energy dependence of the conductance is shown in Fig. 3.4. As it can already be seen from Eq. 3.17, incoming electrons with energies smaller than

<sup>3</sup>This implies  $\tau_{phon} \rightarrow 0$  and thus  $\delta \rightarrow 0$ , which defines the range of validity of our approach.

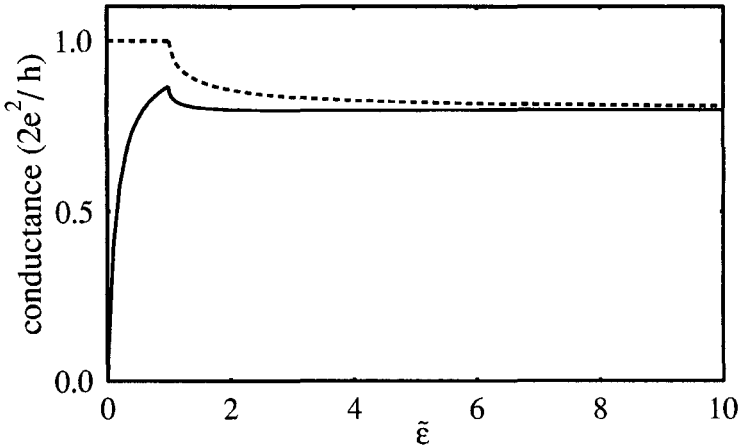


Figure 3.4: Conductance for  $p = 0.1$  in presence of weak elastic backscattering ( $c = 0.15$  in Eq. 3.19). The dotted curve is obtained without backscattering ( $c = 0$ ).

the phonon energy  $\hbar\omega_{phon}$  cannot be scattered into lower-lying states, and the conductance reaches its universal value  $2e^2/h$ , in disagreement with the experiment. This behavior is partly due to our restriction to a single phonon frequency, it will be smoothened when we allow for coupling with the continuum of acoustical phonons, which would also be more realistic. But even this will not affect the value of the conductance at the edge. The remaining discrepancy can be removed by assuming e.g. weak elastic backscattering in the sample region. Near the band edge, the transmission probability in the presence of a thin elastic barrier can be described by

$$T(\tilde{\epsilon}) = \frac{\tilde{\epsilon}}{c + \tilde{\epsilon}} \quad \text{with } \tilde{\epsilon} > 0, \quad (3.19)$$

where  $c \geq 0$  measures the scattering strength of the barrier,  $c = 0$  corresponds to perfect transmission. Fig. 3.4 shows that the conductance peak near the band edge can in fact be suppressed by weak elastic backscattering without affecting the saturation value.

### 3.2.4 Comparison with Experiment and Predictions

In this section we have shown that the nonuniversal conductance plateaus that are observed in thin perfect quantum wires may indicate incomplete Pauli blocking

of electrons entering “occupied” reservoir states. If this picture is correct, the measured step heights should of course depend in a characteristic manner on the system parameters defining the coupling between sample and reservoirs. This expectation is qualitatively confirmed by the experimental facts.

Yacoby *et al.* [16] find that the step height  $\nu$  increases with the widths of the wires. In order to understand this behavior one has to recognize that, in the specific sample geometry used in the experiment, the contact region is the same for all samples, i.e., the ratio between contact surface and volume of the wires decreases for increasing widths of the wires. The sample region, which consists of the wire, is thus gradually closed when the width of the wire is increased. We therefore expect smaller  $p$  values for wide wires, which is in accord with the observed increase of step heights. In fact, the parameter  $p$  is related with the parameter  $\alpha$  in section 3.1.1. The values of the latter were found to be rather small ( $\approx 10^{-6}$ ) in the there-discussed large diffusive systems with small contacts.

Possibly, the increase of the step heights in the presence of a magnetic field perpendicular to the wire found in Ref. [54] may be explained by a similar decoupling mechanism. In this case the effective contact areas are reduced by the formation of edge states. The observed constant step height between consecutive conductance plateaus shows that inter-mode scattering is negligible in the samples of Ref. [16].

Experimentally, the conductance step heights  $\nu$  do not depend on the lengths of the quantum wires for lengths between 1 and 5  $\mu\text{m}$  [16]. For larger lengths the measured conductance decreases and the steps disappear. This experimental behavior is in full agreement with our present description which predicts independence with respect to the sample length as long as multiple elastic scattering can be excluded. Similarly, we also expect different behavior for very short quantum wires, for which the assumption of well defined perfect transmission channels can no longer be justified.

Yacoby *et al.* [16] also find that the step height of the first plateau raises with the temperature in the range  $1\text{K} < T < 25\text{K}$  as well as with the bias. While in Ref. [56] this behavior was attributed to the dependence of the elastic backscattering on the temperature and on the external bias, both situations cannot be treated directly within our two-level approach and their explanation remains a theoretical challenge for further investigations. However, it seems reasonable to assume, that for larger currents the effective width of the contacts reduces due to the charging of the edge states carrying the current. This bottleneck effect would lead to smaller  $p$  values and therefore to larger step heights. Similarly, the thermalization in the reservoirs becoming more rapid with increasing temperature, we would expect that electrons trying to enter the reservoir states from level 2 will

then more and more be hindered by already present reservoir electrons, which have reached these receiving states by inelastic phonon-absorption processes.

The sole existence of nonuniversal conductance steps in quantum wires raises of course the question, under which conditions one will obtain universal rather than nonuniversal behavior. In our model, the situation is controlled by two parameters, the electron-phonon coupling rate in the mesoscopic sample  $1/\tau_{e-ph}$  and the phenomenological parameter  $p$ , which accounts for the contact properties as well as for the diffusion of electrons below the Fermi level in the reservoirs. Universal behavior is only obtained if at least one of these two parameters vanishes, i.e. if  $1/\tau_{e-ph} \simeq 0$  or  $p \simeq 0$ . While of course it will be rather impossible to change the electron-phonon coupling within the wire, it should in principle be possible to follow the transition from nonuniversal to universal behavior by gradually closing the connection with the reservoirs using external gates.

In summary, we state that both behaviors, saturation of  $\tau_\phi$  and nonuniversal conductance steps, may have the same origin. Both effects depend on the effective coupling between the mesoscopic sample system and the surrounding environment. In the mesoscopic regime, more information than given by the usual parameters, such as temperature, sample dimensions and the diffusion constant, is needed to understand the experimental results. In particular, contact parameters that control the openness of the system will play a crucial role in the interpretation of transport experiments.

The approach shown above remains, however, purely phenomenological and gives no clear picture about the microscopical meaning of the parameters  $\alpha$  or  $p$ , which were introduced in a more or less ad-hoc manner. In the next chapters we treat a closed electronic system, which is coupled to the environment via local vibrational degrees of freedom. This way, we strive for a more microscopical approach of the dissipation.



## Chapter 4

# Electron Relaxation in Small Systems

---

The phenomenological description of dissipation, used in the previous chapter, does not relate the chosen parameters to the relevant physical properties of the system. A throughout microscopical treatment of open systems is almost impossible, since the number of intervening system parameters goes to infinity. Unlike an open system, one can describe a closed system completely by the Schrödinger equation. Here we attempt to describe an initially closed small system that is weakly coupled to the environment (e.g. thermally). We consider a finite number of electrons in a finite electronic space. The system is opened in a controllable manner, by introducing indirect interaction processes between the electrons and the environment via internal degrees of freedom of the system. This situation is schematically shown in Fig. 4.1.

The energy relaxation of electrons has been a subject of both experimental (see e.g. [57]) as well as theoretical studies [58, 59, 60, 61, 62]. Using a generalized Monte Carlo approach, Rossi and coworkers have found a strong interplay between energy relaxation and phase coherence [63]. The authors of Ref. [60] investigate the energy relaxation of hot electrons. Assuming a linear energy dispersion they were able to solve exactly the *time-dependent Schrödinger equation*. In the following, we propose a simple method to describe the electron relaxation in a small system with an arbitrary dispersion.

In Ref. [58] the Monte Carlo method is applied to describe the coherent and incoherent phenomena in photoexcited semiconductors. Later, this method is used to investigate the ultrafast carrier dynamics [64, 59], in particular the carrier relaxation and the role of the coherent processes as well as the carrier-carrier processes in Hartree-Fock approximation. The general aim of these authors is to study the phenomena at very short time scales. Our present objective is, however, to achieve an understanding of dissipation and relaxation in the long-time limit,

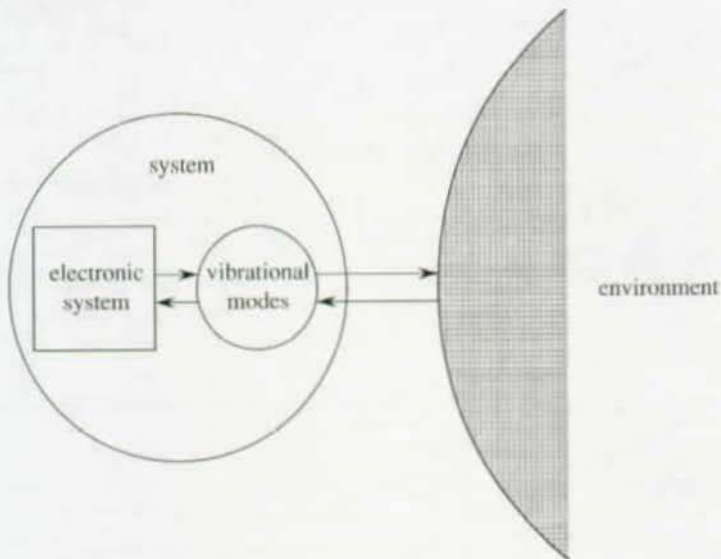


Figure 4.1: Schematic illustration of a closed electronic sample system coupled to the environment via local vibrational modes.

and to describe the electronic dc transport, where the relevant time scales are not of the same order as the reciprocal dissipation rate, but much larger.

## 4.1 Theoretical Model

We investigate the electronic relaxation of a mesoscopic sample, where the electrons are confined to a finite spatial region. The sample form can be chosen arbitrarily. The electrons interact directly with local vibrational modes (LVM) of the sample that can be represented by a certain number of harmonic oscillators. In the absence of the coupling to the environment, no dissipation is expected and the system would completely be described by the Hamiltonian

$$H = H_e + H_p + H_{ep}, \quad (4.1)$$

where  $H_e$  represents the electrons,  $H_p$  considers the LVMs and  $H_{ep}$  is the mutual interaction between both. Depending on the case, one can write down these terms and solve the time-dependent Schrödinger equation. Alternatively, the problem can be solved by studying the time evolution of the density matrix  $\rho$  of the whole

system with the corresponding initial conditions. In this case, one has to solve the Liouville equation

$$\frac{d}{dt}\rho(t) = i[\rho, H] \quad (4.2)$$

instead of the Eq. 2.1. Both methods lead to the same result and the solution can be given in terms of polaronic eigenstates of the Hamiltonian Eq. 4.1.

As long as there is no interaction with the environment, the coherent evolution of the system may be described by either of both methods. The situation changes, when we consider the dissipative processes due to interaction with the environment. While the Schrödinger equation describes merely the coherent evolution of the system, the Eq. 4.2 offers the possibility to extend the description to non-coherent interaction. The most popular way to introduce the decoherence is to add a phenomenological “loss” term to Eq. 4.2 and to study the resulting master equation (see e.g. [65] and the references therein).

Here we introduce dissipation through the coupling to the environmental degrees of freedom. We consider the electron-LVM interaction to be weak and study the problem in the presence of direct coupling between the LVMs and the vibrational modes of the substrate, which are considered to represent an ideal thermal bath. Thus, even for an infinitesimal but non-zero electron-LVM coupling  $H_{ep}$ , the vibrational modes of the isolated mesoscopic system are no more eigenstates of the whole system. This can be accounted for in a phenomenological manner by attributing a finite lifetime  $\tau_p$  to these modes. The coherent evolution of the electrons and the LVMs can only be maintained for times smaller than  $\tau_p$ .

The situation above can be translated into the language of quantum mechanics in the following manner. The Hilbert space  $\mathcal{H}$  of the sample system, containing only electronic and the vibrational degrees of freedom and of the effective dimension  $K$ , is given by the tensorial product between the electronic subspace  $\mathcal{H}_e$  and the vibrational subspace  $\mathcal{H}_p$ ,

$$\mathcal{H} = \mathcal{H}_e \otimes \mathcal{H}_p. \quad (4.3)$$

In the absence of the electron-phonon interaction, the density matrix can be written as

$$\rho(t) = \rho_e(t) \otimes \rho_p(t), \quad (4.4)$$

with

$$\rho_e(t) = \text{Tr}_p \rho(t) \quad (4.5)$$

$$\rho_p(t) = \text{Tr}_e \rho(t), \quad (4.6)$$

being the partial density matrices of the electronic respectively phononic subsystem over the Hilbert subspace  $\mathcal{H}_e$  respectively  $\mathcal{H}_p$ . Eq. 4.4 is no more valid, when

we consider the  $H_{ep}$  term, but one can still define the electronic density matrix  $\rho_e(t)$  (also  $\rho_p(t)$ ) due to Eq. 4.5 (Eq. 4.6). If both systems are weakly correlated (see [66]), the problem can be treated by introducing a correlation term  $\eta_{ep}(t)$

$$\eta_{ep}(t) = \rho(t) - \rho_e(t) \otimes \rho_p(t). \quad (4.7)$$

The coupling to the environment can then be introduced in this picture by tracing over all the LVM states, while the LVM occupation is kept at the thermal equilibrium distribution corresponding to the temperature in the environment.

Here we treat the problem in a similar way. Starting from an initial configuration  $\rho_0 = \rho(t = t_0)$ , the time evolution of  $\rho$  is obtained in a two-step procedure; i) coherent evolution of  $\rho$  during the time interval  $t_0 \leq t \leq t_1 = t_0 + \tau_p$ , and ii) state reduction by tracing  $\rho(t_1)$  over the subspace of LVMs and resetting the LVMs occupations to their equilibrium values. Iterating this procedure, one can then follow the time evolution of the system towards its electronic equilibrium configuration. When the electronic and vibrational subsystems are weakly correlated and at low temperatures, the LVM subspace can be constructed in terms of the ground state and the first excited states of each oscillator. Non-zero temperatures can be treated similarly. Assuming  $M$  harmonic oscillators as the LVMs, the space of the latter is given by all the oscillator states  $|0_i\rangle, |1_i\rangle, \dots, |n_i\rangle$  for  $i = 1, \dots, M$ ,  $|n_i\rangle$  being the highest occupied state of the oscillator  $i$  at the corresponding temperature  $T$ . The electron-LVM interaction, given in general form in Eq. 4.14, couples any oscillator state  $|j_i\rangle$  only to the oscillator states  $|(j-1)_i\rangle$  and  $|(j+1)_i\rangle$ . The Hamiltonian matrix element between the states  $|j_i\rangle$  and  $|(j+1)_i\rangle$  has a prefactor  $1/\sqrt{j+1}$  because of the normalization, i.e. the matrix element becomes less important for the higher excited modes. Thus, the matrix element between the ground and the first excited state has the most weight, even for higher temperatures.

To describe the coherent evolution due to the Eq. 4.2, it is convenient to diagonalize the Hamiltonian  $H$  and change to the eigenbasis, since in this basis the evolution of the density matrix  $\varrho$  is easily calculated by

$$(\varrho(t_1))_{j,k} = \exp(-i(E_j - E_k)\tau_p)(\varrho(t_0))_{j,k}, \quad (4.8)$$

the  $E_j$ 's being the eigenvalues of  $H$  in Eq. 4.1. The density matrix in the product representation of the electronic states and the LVMs, denoted by  $\rho$ , and the density matrix  $\varrho$  in the eigenbasis of the Hamiltonian Eq. 4.1 are related by

$$\varrho(t_0) = S^\dagger \rho(t_0) S, \quad (4.9)$$

where the transformation matrix  $S$  is given by the eigenvectors  $v_i$  of  $H$

$$S = (v_1, v_2, \dots, v_K). \quad (4.10)$$

The trace over vibrational modes Eq. 4.5 in step ii) is most easily calculated in the product basis. Thus, each cycle requires a back- and forth transformation between both basis sets. To be specific, let us consider a single electron in a sample system described by  $N$  electronic states, and interacting with  $M-1$  excited modes of a single oscillator. Then, the density matrix  $\rho$  in the product basis can be written as

$$\left( \begin{array}{cc} \left( \begin{array}{ccc} \rho_{11} & \dots & \rho_{1M} \\ \vdots & \vdots & \vdots \\ \rho_{M1} & \dots & \rho_{MM} \end{array} \right) & \dots & \left( \begin{array}{ccc} \rho_{1K-M} & \dots & \rho_{1K} \\ \vdots & \vdots & \vdots \\ \rho_{MK-M} & \dots & \rho_{MK} \end{array} \right) \\ \vdots & \vdots & \vdots \\ \left( \begin{array}{ccc} \rho_{K-M1} & \dots & \rho_{K-MM} \\ \vdots & \vdots & \vdots \\ \rho_{K1} & \dots & \rho_{KM} \end{array} \right) & \dots & \left( \begin{array}{ccc} \rho_{K-MK-M} & \dots & \rho_{K-MK} \\ \vdots & \vdots & \vdots \\ \rho_{KK-M} & \dots & \rho_{KK} \end{array} \right) \end{array} \right) \quad (4.11)$$

with  $K = M \times N$ . The diagonal elements of each submatrix contain the occupation information of the corresponding vibrational mode. State reduction according to Eq. 4.5 is done by resetting the diagonal elements of each submatrix to the values corresponding to the equilibrium distribution of LVMs and by eliminating the non-diagonal elements.

This iterative procedure is easy to apply, when the number of the electrons and LVMs is small enough. The effective dimension  $K$  of the Hilbert space grows superlinearly with the number of the electrons and that of the LVMs so that an exact diagonalization of the Hamiltonian and back- and forth transformation of  $\rho$  becomes more and more time-consuming. For larger systems, it will be more efficient to switch to the interaction picture and to treat the coherent evolution in second order perturbation theory. In the present work, however, we investigate the physics of small systems, when the direct diagonalization is most convenient.

## 4.2 Single-Electron Relaxation in Small 1D Loops

We first investigate the relaxation of a single electron in a one-dimensional loop. The choice of a loop-formed sample is motivated by the fact that it can later be used to describe electronic transport driven by external fields.

We assume that the sample is embedded in a large gap host material. In the eigenrepresentation,  $H_e$  is given by

$$H_e = \sum_{n=1}^N \epsilon_n c_n^\dagger c_n, \quad (4.12)$$

where the index  $n$  labels the  $N$  eigenstates of  $H_e$  corresponding to the loop, and the operators  $c_n^\dagger$  ( $c_n$ ) denote the respective creation (annihilation) operators. The

electronic system interacts with a single local mode described by  $H_p$

$$H_p = \omega b^\dagger b, \quad (4.13)$$

where  $b^\dagger$  ( $b$ ) denotes the creation (annihilation) operator of the harmonic oscillator with the frequency  $\omega$ . The  $b$  and  $c$  operators obey the commutation or anti-commutation rules for bosons respectively fermions. The mutual interaction between electrons and LVMS has the general form

$$H_{ep} = \sum_{j,k,l} \left( A(j, k, l) c_j^\dagger c_k b_l + B(j, k, l) c_j^\dagger c_k b_l \right). \quad (4.14)$$

As explained before, for the here-assumed weak electron-LVM coupling Eq. 4.14 and zero temperature we can limit the subspace of the LVMS to the first excited state.

$H_e$  is derived from the solution of the  $N$ -site tight-binding Hamiltonian with periodic boundary conditions. Its eigenvalues are given by

$$\epsilon_n = \varepsilon(1 - \cos(k_n)), \quad (4.15)$$

$k_n$  being defined by  $k_n = 2\pi n/N$ , where  $n = -N/2, \dots, N/2$  for even  $N$  or  $n = -(N-1)/2, \dots, (N-1)/2$  for odd  $N$  mark the first Brillouin zone. With the choice Eq. 4.15, the band bottom is at  $n = 0$  and the eigenvalues satisfy  $0 \leq \epsilon_n \leq 2\varepsilon$ . The corresponding eigenfunctions  $|\psi_n\rangle$  can be described in terms of Bloch functions in the basis set of Wannier functions  $|j\rangle$

$$|\psi_n\rangle = \frac{1}{\sqrt{N}} \sum_{j=1}^N \exp(ik_n j) |j\rangle. \quad (4.16)$$

Assuming a constant electron-LVM coupling  $C$  between different electron states, the interaction reads

$$H_{ep} = C \sum_{j,l} c_j^\dagger c_l (b^\dagger + b). \quad (4.17)$$

It might appear that the description of the local vibrational modes by a single oscillator is too rudimentary to investigate the evolution of the system. However, this rather simplified model yields all the essential features of more elaborated descriptions, which include more oscillator states. In particular, it is sufficient to discuss the role of different parameters included in the model.

## 4.2.1 Numerical Results

In the following we assume Rydberg atomic units (au) for the energies. The corresponding time unit is  $\tau_0 = 4.484 \times 10^{-17} \text{ s}$ <sup>1</sup>. As an example we consider the

<sup>1</sup>see e.g. Journal of Physical and Chemical Reference Data, Vol 28, No.6, (1999). The value given there corresponds to Hartree units for the energy, and has to be multiplied by a factor of two for the here-assumed Rydberg units

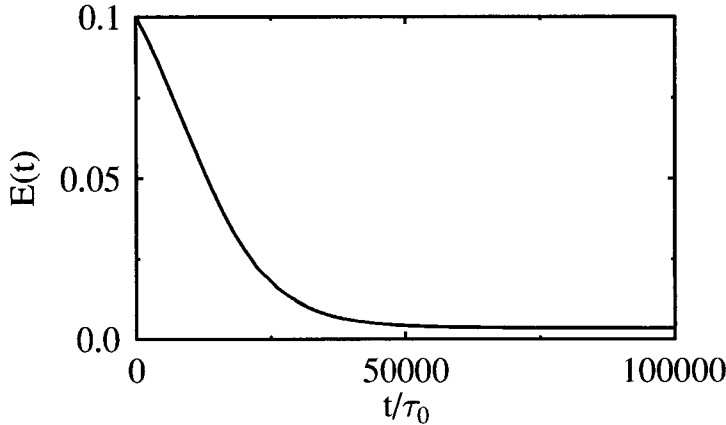


Figure 4.2: Energy relaxation of a single electron in a loop with respect to time. The electronic system is described by  $N=20$  states and  $\varepsilon = 0.05$  au. The latter are coupled to a single mode of frequency  $\omega = 0.01$  au, with coupling factor  $C = 0.0005$  au and  $\tau_p = 400\tau_0$ .

energy relaxation of an initially excited electron in a loop with  $N = 20$  sites and  $\varepsilon = 0.05$  au. The initial state of the excited electron is chosen to be the uppermost state of the band.

The relaxation depends of course on the choice of the oscillator Eq. 4.13, defined by  $\omega$ , on its coupling to the electronic states  $C$ , and on the parameter  $\tau_p$ , which describes the interaction with the environment. The relaxation behavior of the electron is characterized by the time dependence of its energy

$$E(t) = \text{Tr}(\rho_e(t)H_e) \quad (4.18)$$

and by the corresponding occupation number, which is given by the diagonal elements of the electronic density matrix  $\rho_{e,ii}(t)$ ,  $i = 1, \dots, N$  at different times. An example is shown in Fig. 4.2. A nearly perfect relaxation into the ground state is achieved with the parameter set  $\omega = 0.01$  au,  $C = 0.0005$  au and  $\tau_p = 400\tau_0$  after about 2.5 ps.

Fig. 4.3 shows that the electron wave packet spreads over all the electronic states at intermediate times before it localizes finally over the three states with

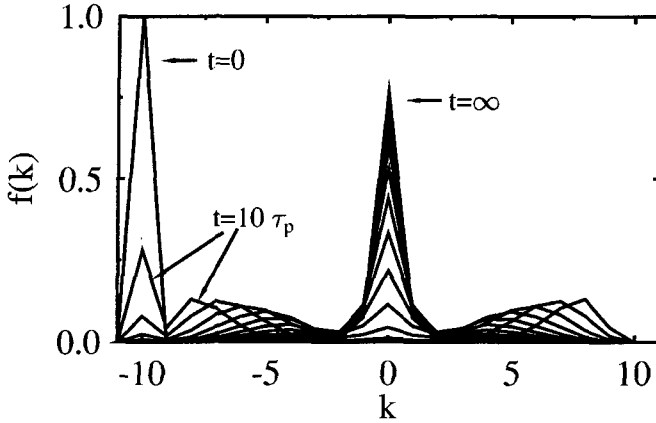


Figure 4.3: Occupation of electronic states for the same parameter set as for Fig. 4.2 at different times  $t = n\tau_p$ ,  $n = 0, 10, 20, \dots$

the lowest energy. We note that the relaxation cannot be described within the approach of Fermi's golden rule. With the choice of a finite value of the parameter  $\tau_p$  one excludes all trivial blockings due to the eventual mismatch between  $\omega$  and the energy difference between two electronic eigenstates, and it becomes possible to describe the electronic relaxation even for a strongly energy-dependent density of states, as it is the case for the tight-binding band.

The final electronic energy after relaxation

$$E_\infty = \lim_{t \rightarrow \infty} E(t) \quad (4.19)$$

may be used to illustrate the effect of the model parameters. In particular,  $\tau_p$  controls the coupling of different electronic states to the ideal bath representing the further environment. In the extreme limit  $\tau_p \rightarrow 0$  there is no energy conservation at all. Hence, all electronic states are equally coupled to each other. In the long-time limit the occupation of each state becomes thus independent of its energy so that

$$\rho_{e,ii}(t \rightarrow \infty) = \frac{1}{N} \quad \forall i \quad \Rightarrow \quad E_\infty = \varepsilon. \quad (4.20)$$

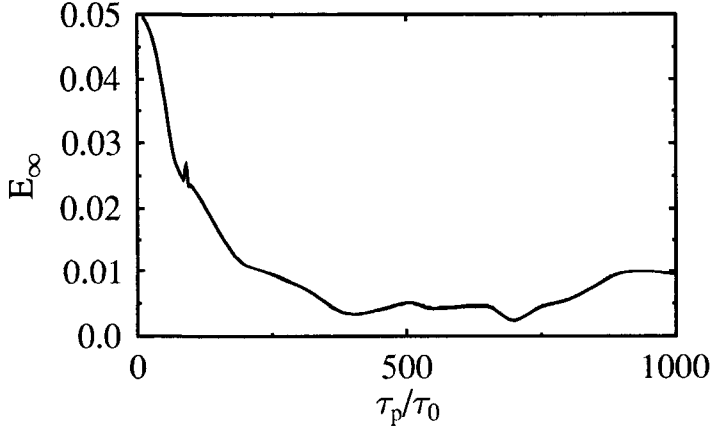


Figure 4.4: Final electronic energy as a function of the lifetime  $\tau_p$  of the oscillator states. The other parameters are the same as in Fig. 4.2.

The opposite limit  $\tau_p \rightarrow \infty$  describes the case of vanishing coupling to the environment. The relaxation slows gradually down in this limit. The case  $\tau_p = \infty$  corresponds to the coherent evolution of the electron-LVM system. As it can be seen in Fig. 4.4,  $E_\infty$  remains more or less unchanged for a long range between these two limits, passing through a minimum for an intermediate  $\tau_p$ . We note that our approach is only adequate to describe the time evolution of  $\rho(t)$  for times  $t > \tau_p$ .

The dependence of  $E_\infty$  on the oscillator frequency  $\omega$  is demonstrated in Fig. 4.5. Again the two limiting cases  $\omega \rightarrow 0$  and  $\omega \gg 2\varepsilon$  can easily be understood. Up- and downward coupling become the same when  $\omega$  tends to zero, leading to the situation described by Eq. 4.20. Similarly when  $\omega \gg 2\varepsilon$ , the coupling between the electronic states becomes uniform and  $E_\infty$  approaches in this case monotonously the mid-band value  $\varepsilon$ . For  $0 < \omega < 2\varepsilon$ , the final electron energy fluctuates with  $\omega$  as a result of its coincidental resonance with the electronic transition energies at the bottom of the band.

Other more microscopical models for the local vibrational modes are given and discussed in Ref. [67], such as coupling to several ( $M$ ) local oscillators with the

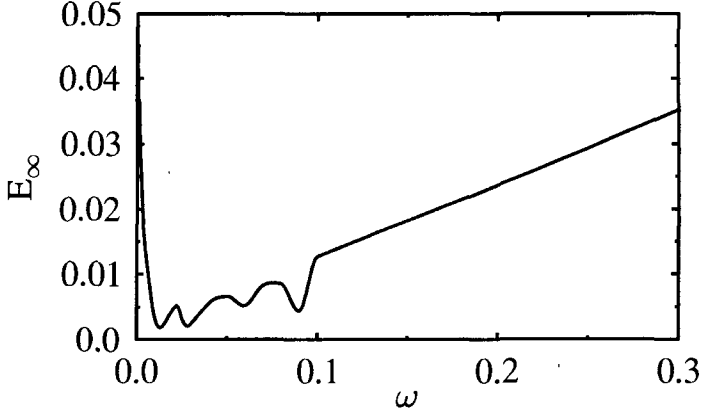


Figure 4.5: Final electronic energy as a function of the frequency of the single mode  $\omega$ . The other parameters are the same as in Fig. 4.2.

same frequency, where

$$H_p = \omega \sum_{j=1}^M b_j^\dagger b_j \quad (4.21)$$

$$H_{ep} = C \sum_{j,k,l} c_j^\dagger c_k (b_l^\dagger + b_l), \quad (4.22)$$

or the coupling to the acoustical phonons in the Debye model, represented by

$$H_p = \sum_{q \neq 0} \omega_q b_q^\dagger b_q \quad (4.23)$$

$$H_{ep} = iC \sum_{k,q} (2q/N)^{\frac{1}{2}} c_{k+q} c_k (b_q - b_{-q}^\dagger) \quad (4.24)$$

with  $q = [-\frac{N}{2}], \dots, [\frac{N}{2}]$  and  $\omega_q = 2\omega_D |q|/N$ .

Figures 4.6 and 4.7 show the time dependence of the electronic energy and the occupation of the states for different times using equations 4.23 and 4.24. Comparison of Figures 4.2, 4.3 and 4.6, 4.7 shows that the SM approach is quite sufficient to describe the essential features of the electronic relaxation. For general

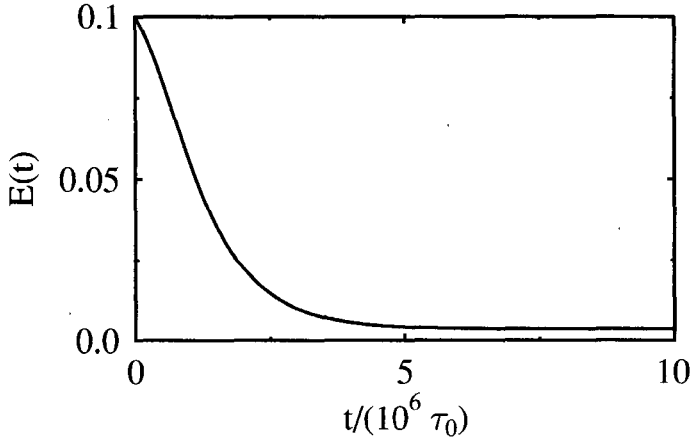


Figure 4.6: Time dependence of the energy relaxation for the same electronic system as in Fig. 4.2 coupled to acoustical phonons. The latter are described by the parameters  $\omega_D = 0.015$  au,  $C = 0.0001$  au and  $\tau_p = 10^4 \tau_0$ .

consideration, it is thus possible to use the SM approach instead of a much more cumbersome many-mode approach. The price to pay is that no direct microscopical meaning can be attributed to the parameters used in the SM approach. The parameter set, however, can be chosen to simulate the results of more microscopical models without the considerable numerical effort, needed for the latter.

In our model description, the dissipation is due to the contact to the environment. Electrons in the system interact coherently with the LVMs giving energy to the vibrational subsystem. The energy gained by the LVMs is then absorbed by the further environment. The non-diagonal elements of the density matrix Eq. 4.11 contain the information about the phase coherence between the different states. While resetting  $\rho(t)$  to its equilibrium values, the vibrational subsystem loses its phase coherence as well as its energy. The phase coherence between different electronic states remains, however, untouched by the state reduction.

Another aspect of our results is that the final stationary state of a relaxing electronic system is not perforce its ground state. Here we may distinguish between *bottleneck effects* that retard the relaxation and *environmental blockings*

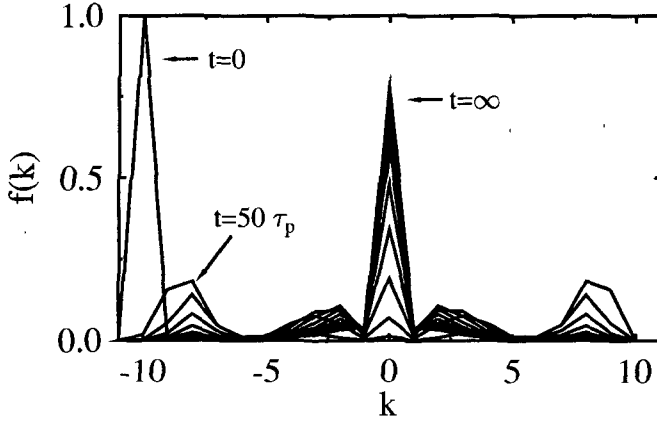


Figure 4.7: Occupations of electronic states for the same parameter set as for Fig. 4.6 at different times  $t = n\tau_p$ ,  $n = 0, 10, 20, \dots$

that cause the stationary state of the system to be different from the ground state.

### 4.3 Two-Electron Relaxation

The simplest non-trivial case to look at the effect of interactions between the electrons is a two-electron system. In fact, various characteristics of a many-electron system can already be studied in a two-electron system, thus avoiding long calculations, which would be necessary for many-electron systems. In the following, we use the iterative procedure, described in Section 4.1, to determine the time evolution of the electronic density matrix corresponding to two relaxing electrons in the small 1D loop.

The Hamiltonian of the confined electronic system interacting with LVMs reads

$$H = H_c + H_p + H_{cp} + H_{ee}, \quad (4.25)$$

where  $H_e$  is the non-interacting electronic Hamiltonian defined by

$$H_e = \sum_k \epsilon_k c_k^\dagger c_k. \quad (4.26)$$

$H_p$  and  $H_{ep}$  are given according to the set of LVMS. As demonstrated in the previous section, relaxation can be accessed at least qualitatively within the SM approach, thus avoiding unnecessary numerical effort. Only the parameter set has to be adapted to the problem. In the following we dispose of the parameters in Equations 4.13 and 4.14.

The Hamiltonian describing the electron-electron interaction in  $\mathbf{q}$  representation is given by

$$H_{ee} = \frac{1}{2} \sum_{k_1, k_2, q} V_q c_{k_1}^\dagger c_{k_2}^\dagger c_{k_2+q} c_{k_1-q}, \quad (4.27)$$

where  $V_q$  describes the Coulomb potential. In the  $\mathbf{r}$  representation,  $H_{ee}$  reads

$$H_{ee} = \sum_{\mathbf{r}_1, \mathbf{r}_2} \frac{\alpha}{|\mathbf{r}_1 - \mathbf{r}_2|}, \quad (4.28)$$

where  $\alpha$  includes all other constants. This potential is evaluated for our special geometry of a loop in Appendix A.

We distinguish between the case of electrons with parallel spins and that of electrons with opposite spins.

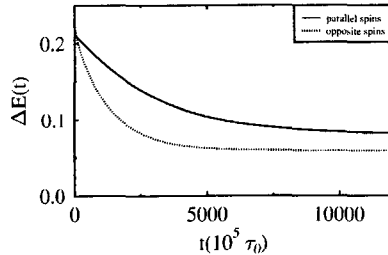
### 4.3.1 Pauli Exclusion

We first study the relaxation for non-interacting electrons ( $H_{ee} = 0$ ). The number of two-electron states increases quadratically with the number of one-electron states, i.e.  $N(N-1)/2$ . In order to limit the numerical effort we choose in the following  $N = 10$  states. The energy dispersion of the electrons is given by Eq. 4.15 and  $\varepsilon = 0.06$  au, the frequency of LVM being  $\omega = 0.01$  au and the coupling factor  $C = 0.0003$  au. Starting from the uppermost excited electronic levels, in which the electrons occupy the uppermost electronic states of the non-interacting system, we follow the relaxation of the electronic system. Fig. 4.8 shows the time-dependence of the electronic energy with respect to the ground state  $\Delta E(t) = E(t) - E_G$ , with  $E_G$  being the ground-state energy of the pure electronic system for the respective spin configuration.  $\Delta E_\infty$  is defined accordingly by

$$\Delta E_\infty = \lim_{t \rightarrow \infty} \Delta E(t). \quad (4.29)$$

The case of electrons with opposite spins is calculated assuming independent relaxation of the two electrons. This simplification means, strictly spoken, that each electron is connected to a different vibrational mode so that we are not

Figure 4.8: Two-electron energy relaxation in a ring with  $N = 10$  electronic sites and  $\varepsilon = 0.06$  au, coupled to a single vibrational mode. The latter is defined by the parameter set  $\omega = 0.01$  au,  $C = 0.0003$  au and  $\tau_p = 10^5 \tau_0$ . The solid line represents the case of electrons with parallel spins. The dotted line depicts the relaxation of two independent electrons that can be interpreted to represent the case of opposite spins (see text).



exactly in the same situation as in the case of the electrons with parallel spins, where two-electron states are connected to a common single mode. However, for the considered weak electron-LVM coupling  $C$  the effective interaction between the electrons via LVM is negligible, and the results become comparable.

According to the Pauli exclusion principle, two electrons with parallel spins cannot occupy the same state, hence an electron is hindered to enter into a state already occupied by the other. Fig. 4.8 shows the results for the case, where bottleneck effects are negligible. The comparison of the energy relaxation for both spin configurations shows that the two electrons with *opposite* spins relax faster, and  $E_\infty$  comes closer to the ground state value. This is, however, not a general result. The parameter set of Fig. 4.8 is chosen so that the relaxation is almost perfect for each electron. The relaxation of two electrons with *parallel* spins can even be faster, and their final state may come closer to the ground state, when bottleneck effects in the single-electron relaxation are important. This may seem strange at the first glance, but it can be explained by the fact that the Pauli exclusion principle hinders the electrons to enter certain states, which act eventually as temporary traps, and so it helps to bridge the bottlenecks.

### 4.3.2 Electron-Electron Interaction

In the previous subsection, we have treated the electrons as chargeless particles. We now study the influence of the Coulomb interaction between the electrons on the relaxation. The electron-electron interaction is scaled through an additional parameter  $\alpha/R$ , where  $R$  is the radius of the ring (see Appendix A).

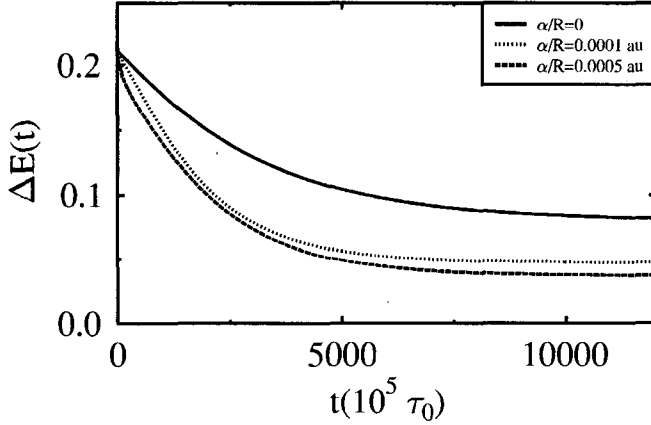


Figure 4.9: Time dependence of  $\Delta E$  (see text) for a two-electron system with parallel spins and different Coulomb interaction strengths between the electrons. The electronic and vibrational parameters are the same as in Fig. 4.8.

Figures 4.9 and 4.10 show the energy relaxation of two electrons with parallel, respectively opposite, spins for the same case as before, but for electron-electron interaction parameters  $\alpha/R = 0.0001$  and  $0.0005$  au. Weak electron-electron interaction facilitates the relaxation of electrons. For both spin configurations and in the limit of small  $\alpha/R$ -values,  $\Delta E_\infty$  decreases with increasing parameter  $\alpha/R$ , and the relaxation into the stationary state becomes faster. If we continue to increase the interaction,  $\Delta E_\infty$  passes through a minimum and finally it starts rising to higher values. For rising Coulomb interaction, the relaxation time increases as well. This can be seen in Fig. 4.11, where we compare  $\Delta E(t)$  for  $\alpha/R = 0.001$  au and  $\alpha/R = 0.0005$  au with the relaxation of interaction-free electrons with parallel spins.

In order to understand the above mentioned effects one has to consider the dependence of the eigenvalue spectrum of the electrons on the Coulomb interaction. Fig. 4.12 shows the energy levels of the two-electron system with the same electronic parameter set as in Fig. 4.8 and for different  $\alpha/R$ . Introducing a weak electron-electron interaction, the degeneracy of the states is removed without a noticeable change in the difference between minimum and maximum of the

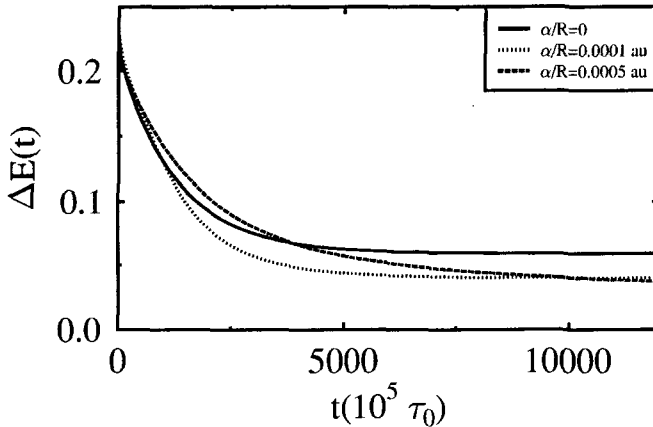


Figure 4.10: Time dependence of  $\Delta E$  (see text) for a two-electron system with opposite spins and different Coulomb interaction strengths between the electrons. The electronic and vibrational parameters are the same as in Fig. 4.8.

energy eigenvalues. This reduces the energetic distance between adjacent states and facilitates the relaxation. In principle, the coupling of the non-interacting two-electron states should also lead to a more uniform coupling of the resulting eigenstates of the interacting system with the oscillator. This effect, which would also enforce the above tendency, intervenes only when the electron-LVM coupling matrix elements depend on the electronic states, and it does not exist for the here-considered state-independent  $C$ . Further increase of the Coulomb interaction leads to a separation of the energy levels, so the relaxation decelerates gradually and more time is needed to attain the stationary state. This behavior is found for both spin configurations.

Before passing to the next chapter we want to stress that the final stationary state can be different from the ground state. This difference cannot be attributed to the fact that the calculation is in practice interrupted at long times. Fig. 4.13 shows  $\Delta E(t)$  for two interacting electrons with parallel spins, the same electronic and vibrational parameter sets as in Fig. 4.9, and  $\alpha/R = 0.0005$  au. The solid line represents the relaxation from the uppermost electronic state, while the initial state for the dotted curve is the ground state of the system. The stationary state

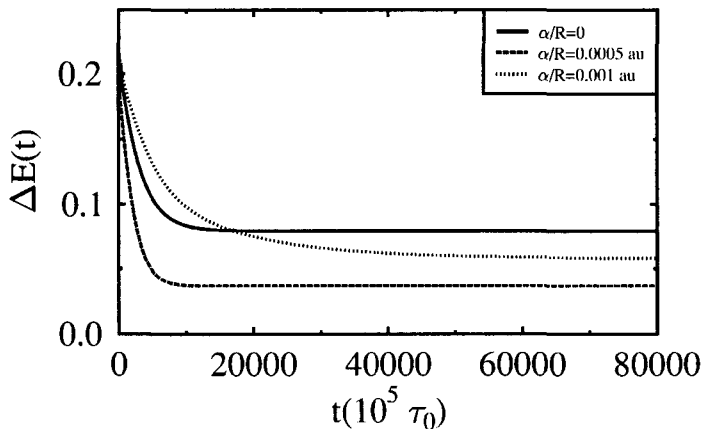


Figure 4.11: Time dependence of  $\Delta E$  for a two-electron system with parallel spins. The electronic and vibrational parameters are the same as in Fig. 4.8.

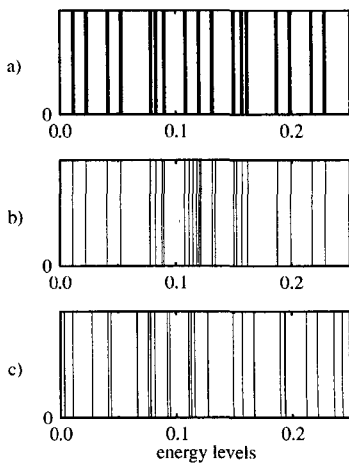


Figure 4.12: Energy eigenvalues of the two-electron system with parallel spins from Fig. 4.8 without electron-electron interaction (a) in comparison to the cases with the electron-electron interaction: b)  $\alpha/R = 10^{-4}$  au and c)  $\alpha/R = 5 \times 10^{-4}$  au.

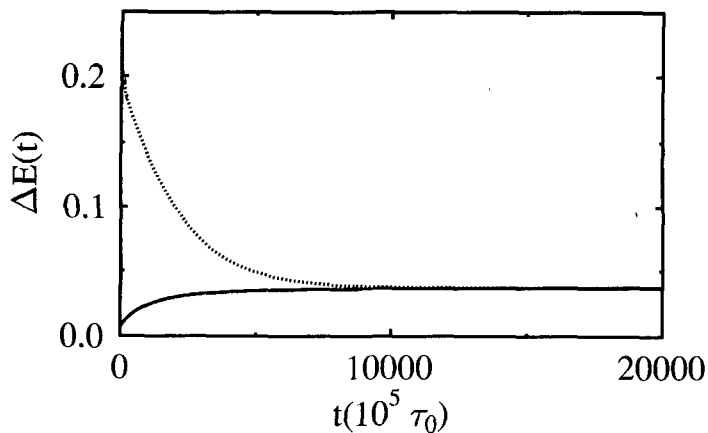


Figure 4.13: The stationary state does not depend on the initial state. Starting from the ground state (solid line) or the uppermost state (dotted line) the relaxation process leads to the same final state, which is different from the ground state.

for both cases is the same, and so it is independent of the initial state. This is true for all the relaxation situations shown here.

# Chapter 5

## Persistent Currents

---

Small ring systems provide an excellent testing ground to gain insight into some basic aspects in mesoscopic physics. Considering a ring threaded by a constant magnetic flux  $\phi$ , and inspired by the fact that the periodicity of the potential on a ring makes the problem formally the same as that of Bloch wave functions in a crystal, Büttiker, Imry and Landauer have predicted that this should lead to a persistent current in the electronic ground state [68]. The persistent current in rings is periodic with respect to enclosed flux with the period  $\phi_0 = hc/e$ . Later, Landauer and Büttiker have shown that neither finite temperature nor elastic scattering will destroy the effect and that the latter can also survive weak inelastic scattering [69].

Though persistent currents have been discussed theoretically by many authors [70, 71], no experimental evidence of their existence was provided until the beginning of the nineties. Lévy and coworkers have first measured persistent currents of  $10^7$  isolated copper rings [72] at low temperatures and found a  $\phi_0/2$  (and not  $\phi_0$ ) periodicity of the currents. Somewhat later, another group gave account about their measurements on single Au loops [73]. The authors found that the current oscillates with a period  $\phi_0$ . Moreover, both groups reported values for the persistent current, which are 1 to 2 orders of magnitude larger than the ones theoretically predicted. Other authors, who have measured the persistent currents in a single GaAs/AlGaAs loop, however, have found a current amplitude in good agreement with the theoretical prediction [74]. While the reason for  $\phi_0/2$  oscillations are more or less well understood [71], no definitive explanation for the discrepancy between the theoretical and experimental values has yet been found.

In the following, we study persistent currents within the scope of our approach. The role of electron-electron interactions is investigated in a two-electron system. We discuss also the effects of bottlenecks and incomplete relaxation on the persistent currents.

## 5.1 Persistent Currents in the Electronic Ground State

After a revolution around a one-dimensional (1D) ring an electron reaches exactly the same point as before. Thus, the electrons in a ring behave the same as the ones in a periodic potential. The wave vectors, comparable to Bloch wave vectors in a crystal, are given by  $k_n = 2\pi n/N$ , where  $N$  is the number of the sites on the ring. In the presence of a magnetic flux, one can treat the problem by introducing the corresponding vector potential  $\mathbf{A}$  in the Hamiltonian or by solving the problem for modified boundary conditions [75]. Choosing the second way, the wave vector  $k_n$ , determined by the flux-dependent boundary conditions, then reads

$$k_n = \frac{2\pi}{N} \left( n + \frac{\phi}{\phi_0} \right). \quad (5.1)$$

On the other hand the current operator in a 1D system is given by

$$\hat{j} = e \frac{\partial \hat{x}}{\partial t} = e \frac{i}{\hbar} [H, \hat{x}]. \quad (5.2)$$

Changing into the momentum representation we obtain

$$\hat{j}_k = \frac{e}{\hbar} \left[ H, \frac{\partial}{\partial k} \right]. \quad (5.3)$$

The expectation value of the current is then easily calculated from

$$I_k = -\frac{e}{\hbar} \frac{\partial E(k)}{\partial k}. \quad (5.4)$$

Replacing  $k_n$  in Eq. 4.15 by the one given in Eq. 5.1 we calculate the ground state of a ring exposed to a magnetic flux  $\phi$  by diagonalizing the Hamiltonian in the two-electron basis. The current operator, however, is a one-electron operator. The total current in the ring is given by the sum of the partial currents of each state  $k_n$ , the latter being the product of the state current Eq. 5.4 and the corresponding occupation of the state. In the operator form, the total current reads

$$I_{tot} = Tr(\rho_e \hat{j}), \quad (5.5)$$

where  $\rho_e$  is defined by Eq. 4.5. Eq. 5.5 can be simplified to

$$I_{tot} = \sum_k \rho_e^k I_k, \quad (5.6)$$

$\rho_e^k$  being the occupation of the one-electron state with the wave vector  $k$ .

Figure 5.1: Persistent currents of the two-electron ground state with parallel spins in a 10-site ring. The band width is  $2\varepsilon = 0.12$  au. No other interaction is included.

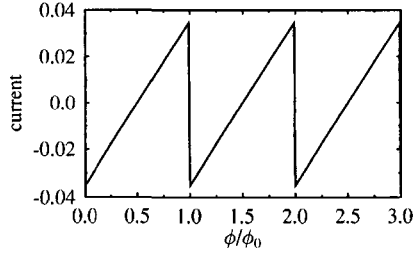


Figure 5.2: Persistent currents of the two-electron ground state for different electron-electron strengths. The electronic parameters are the same as in Fig. 5.1. The electron-electron parameter is increased from  $\alpha/R = 0$  (solid line) to  $\alpha/R = 0.008$  au (dotted line) and further to  $\alpha/R = 0.0015$  (dashed line).

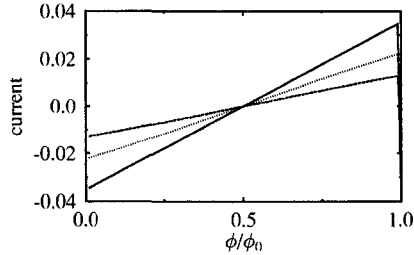


Fig. 5.1 shows the periodic ground state current of two electrons with parallel spins in a loop with  $N = 10$  sites and  $\varepsilon = 0.06$  au, neglecting the Coulomb interaction.

In the next step we study the effect of Coulomb interaction between the electrons on the ground-state current. Assuming the Hamiltonian Eq. 4.25, we calculate the ground-state current of the loop for different electron-electron interaction strengths. The persistent currents with respect to the flux are shown in Fig. 5.2 for the parallel spin configuration. The solid line represents the case of non-interacting fermions,  $\alpha/R$  is given by 0.0008 au or 0.0015 au for the dotted, respectively dashed diagram. We notice that the persistent current of the ground state is progressively suppressed by the electron-electron interaction. This is an artifact of the tight-binding model. The Coulomb interaction couples between all non-interacting two-electron basis states. In the limit of very strong interaction all states are equally coupled as a result of the limited band width so that the ground state of the system contains all two-electron basis states with the same weight. This can be compared with the situation of a full band, which carries no current.

The effect of electron-electron interaction can also be understood in a perturbation theory argumentation: The Hamiltonian  $H = H_e + H_{ee}$  can be divided by the factor  $\alpha/R$  that scales the Coulomb interaction. When the latter is sufficiently large, the other contributions to the Hamiltonian  $H_e$  can be treated as a perturbation. In the limit  $H_{ee} \rightarrow \infty$ ,  $H_e$  becomes negligible, and the problem can be treated as if  $2\varepsilon \rightarrow 0$ , which corresponds to the case of zero band width. Thus, the total current, being related to the band width by Equations 5.4 and 5.6, is expected to vanish in this limit.

The arguments given above are of course not valid for an unlimited spectrum, as e.g. in the free-electron approximation. The persistent currents and the role of the electron-electron interaction in such cases are discussed in Ref. [76].

## 5.2 Persistent Currents in Presence of Environmental Coupling

In this section we investigate the persistent currents of a ring, where the latter is coupled to the environment in the same manner as was described in Chapter 4. Again we assume two electrons on a ring of  $N = 10$  sites and change step by step the magnetic flux. For each step we calculate first the final stationary electronic configuration  $\rho_e(t = \infty)$ . The corresponding current is then obtained from Eq. 5.5. We have checked that the current is independent of the initial conditions.

Fig. 5.3 shows the calculated current as a function of the flux over a period  $\phi_0$  for two electrons with parallel spins in a band of half width  $\varepsilon = 0.06$  au. The electron-electron interaction is here neglected. The parameter set involving the single LVM is  $\tau_p = 300\tau_0$ ,  $\omega = 0.013$  au and  $C = 0.0003$  au. Passing through  $I(\phi_0/2) = 0$ , fixed by the symmetry of the problem, the current-flux diagrams of the relaxing system show the expected  $I(\phi + \phi_0/2) = -I(-\phi + \phi_0/2)$  relation. The difference between the current of the relaxing system (solid line) and the persistent currents of the ground state (dashed line) is due to the fact that the system does not reach its true electronic ground state.

Obviously, it is impossible to find a parameter set for a single mode that allows a perfect relaxation of the electrons into the ground state over the whole flux range. The relaxation of the electrons becomes the more difficult, the more the electronic states approach each other. So, the relaxed electrons spread over several low-energy states at the bottom of the band instead of being localized in the true electronic ground state. Qualitatively, it can be stated that persistent currents of the ground state can only be expected, if the LVMs, which are available to the system, couple between the energetically deepest states to allow perfect relaxation between adjacent levels. Once the origin of the difference is understood,

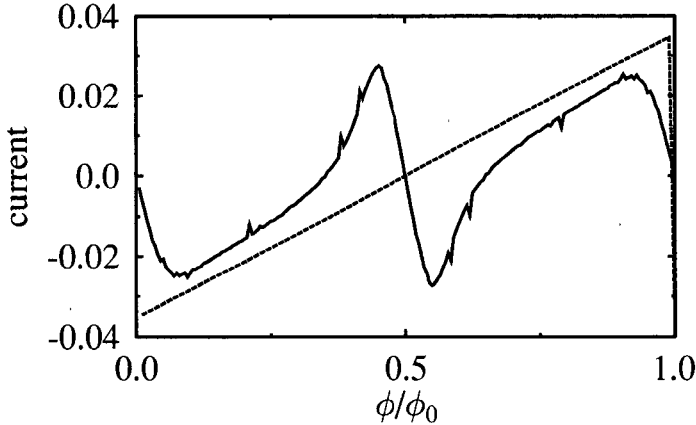


Figure 5.3: Currents of a relaxing two-electron system (solid line) in comparison to ground state currents (dashed line). The electronic parameters are the same as in Fig. 5.1. The single vibrational mode of the relaxing system is described by  $\omega = 0.013$  au,  $C = 0.0003$  au and  $\tau_p = 300\tau_0$ .

the question has to be raised about the existence of these environmental blockings in real systems. Are they only artifacts of our approach or can one expect such effects even in real experiments?

In order to give an answer to this question it is sufficient to discuss the influence of different parameters on the relaxation. As it was mentioned in Subsection 4.2.1, in the single-mode approximation the parameters like  $\omega$  and  $\tau_p$  do not correspond to the true microscopic values of the system. Nevertheless, these model parameters can be chosen to describe qualitatively different cases that can occur in real experimental situations. The oscillator frequency  $\omega$  is the essential parameter that influences the current-flux dependency. The current-flux diagrams for different  $\omega$  values are shown in Fig. 5.4. All other parameters are the same for all the curves, in particular  $\tau_p = 300\tau_0$  is chosen small enough so that there are no dynamical bottlenecks. The best correspondence with the ground state curve is achieved if the oscillator frequency is adapted to the energy difference between the ground state and the first excited states  $\Delta E_1$ , i.e.  $\omega \approx \Delta E_1$ . The curves get even closer if one adds one or more oscillators with smaller frequencies to the system.

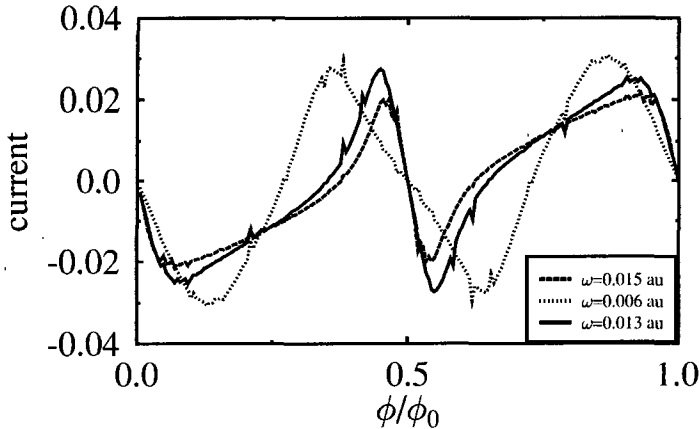


Figure 5.4:  $\omega$  dependence of the persistent currents in a relaxing system in contact with the environment. The corresponding  $\omega$  values are given in the inset. All the other parameters are the same as in Fig. 5.3.

A rough estimation yields the relation between  $\Delta E_i$  and the relevant phonon energies of a real system. For a metal loop at zero temperature the problem can be reduced to an effective two-level model, since all the states below the Fermi level  $E_F$  are occupied. Hence, we need to estimate the level differences  $\delta E$  in the neighbourhood of the  $E_F$ . Assuming a quadratic dispersion  $E = k^2$ , one deduces

$$\delta E|_{k=k_F} = 2k_F \delta k. \quad (5.7)$$

For a ring of the perimeter  $L = 10 \mu\text{m}$  (which is the approximative length of the loops in Ref. [73]) and  $E_F = 1 \text{ eV}$ ,  $\delta k = 2\pi/L$  and  $k_F = \sqrt{E_F}$  can easily be estimated and we find according to Eq. 5.7  $\delta E \approx 0.3 \text{ meV}$ , which is much smaller than the phonon-energies of optical phonons of the order 10-100 meV.

The rough estimation above shows that environmental blockings have to be expected in experimentally relevant situations. In the following, we discuss some particular effects of *incomplete* relaxation.

## 5.3 Higher Harmonics

The authors of Ref. [72] reported a  $\phi_0/2$  dependence of the persistent currents for their  $10^7$  copper rings. The later observations of the persistent currents of a single loop confirmed the predicted  $\phi_0$  oscillations [73]. The reason of this discrepancy is attributed to the ensemble averaging in Ref. [77]. In fact, the persistent currents are shifted by  $\phi_0/2$  depending on the odd or even number of electrons in the ring. The number of electrons being randomly odd or even for each isolated ring, the  $\phi_0$  contribution averages out to zero for the large number  $10^7$ , while the  $\phi_0/2$  contribution remains non-zero.

The current-flux diagram for  $\omega = 0.006$  au in Fig. 5.4 (dotted line) shows a case, where the even superharmonics dominate the flux dependence of the current and where the  $\phi_0/2$  oscillation is clearly visible. All other parameters are the same as in Fig. 5.4. As the calculations are performed for a single loop without disorder, the reason for the  $\phi_0/2$  oscillation cannot be attributed to ensemble averaging. In fact, the  $\phi_0/2$  oscillation found in our calculations is due to the contributions of excited electronic states. The occupation  $p_e^k$  of the electronic states and their individual contributions  $I_k$  to the current are both periodic in the magnetic flux with the period  $\phi_0$ . The product in Eq. 5.6 leads then to the appearance of the higher harmonics. However,  $\phi_0/2$  harmonics remain the dominating terms.

Our results indicate that the coupling of the sample to the environment should explicitly be taken into account to get a correct understanding of the experimental results. In particular, it cannot be expected that the relaxed electronic configuration of the coupled sample system reaches the ideal electronic ground state of the isolated sample. A ground state theory is only applicable, when the LVM coupling obeys very strict conditions, which cannot be expected to be realized in true experimental situations.

### 5.3.1 Persistent Currents of Interacting Electrons

We introduce the Coulomb interaction in the same manner as it was described in Section 4.3 and look at the persistent currents of the system for different interaction strengths in the case of two electrons with parallel spins (Fig. 5.5). In order to get comparable results, the same parameter set as in Fig. 5.3 is used here. Comparison between Fig. 5.3 and Fig. 5.5 shows that the jump of the current at  $\phi = 0$  is smoothed by the electron-electron interaction. This is due to the state mixing in the presence of the Coulomb interaction. The currents of the relaxing system deviate maximally from that of the ground state around  $\phi = \phi_0/2$ , where the relaxation into the ground state becomes more difficult because of the degeneracy of the contributing one-particle states. For increasing strength of the

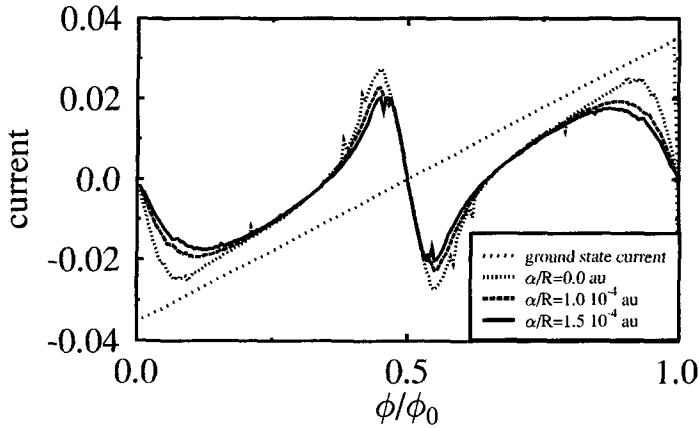


Figure 5.5: Comparison between the persistent currents of the same relaxing electronic system as in Fig. 5.3 for different electron-electron interaction strengths. The curve for the ground-state current is valid for all interaction parameters in the considered case.

Coulomb interaction, the current approaches the ground state current, as long as the interaction is weak enough. This confirms our previous results in Chapter 4, where we have found that weak Coulomb interaction facilitates the relaxation towards the electronic ground state.

The persistent currents become smaller at any  $\phi$ , when the Coulomb interaction is further increased, in agreement with the discussion in Section 5.1.

## Chapter 6

# Transport in Loops Coupled to Their Environment

---

There are two ways to obtain a dissipative direct current in a lead. One of them is assumed in the Landauer picture of transport, in which the current through the lead is driven by the difference in the chemical potentials of the two connected reservoirs. The second way is to generate the current in a ring threaded by a time dependent magnetic flux. If the latter increases linearly in time, and in the limit of strong dissipative coupling, one expects a direct current driven by the corresponding electromotorical force (EMF).

The current generated by a constant EMF is, however, not necessarily a direct current. In a full coherent loop system, the electrons are expected to travel through the electronic band leading to an oscillatory behavior of the current [78, 79], known as Bloch oscillations. Experimentally, Bloch oscillations have been observed only recently, mostly for photoexcited carriers in semiconductor superlattices [80, 81, 82]. The oscillations are damped in the presence of dissipative interactions between the system and the environment.

In this chapter we extend our model to describe the transport in a small loop pierced by a flux increasing linearly with time. Controlling the openness of the system through our model parameters, we then cover in principle the whole transport regime from the coherent carrier transport and Bloch oscillations up to the Ohmic regime.

### 6.1 Sudden Approximation

The situation of a time-dependent flux can be described using the so-called acceleration theorem [75]

$$\frac{d\mathbf{k}}{dt} = e\mathbf{E}, \quad (6.1)$$

where  $\mathbf{E}$  represents the electric field. On the one hand, according to Maxwell equations the vector potential  $\mathbf{A}$  is related to electric field by

$$\mathbf{E} = -\frac{1}{c} \frac{\partial \mathbf{A}}{\partial t} \quad (6.2)$$

so that the vector potential  $\mathbf{A}$  corresponding to a constant  $\mathbf{E}$  is given by  $\mathbf{A} = -c\mathbf{E}t$ , where  $c$  denotes the speed of light. On the other hand, the vector potential and the flux, being related by

$$\phi = \oint \mathbf{A} d\mathbf{r}, \quad (6.3)$$

have the same time dependence, so we can apply Eq. 6.1 for a constant electric field to describe a ring threaded by a magnetic flux increasing linearly in time  $\phi(t) = \gamma t$ ,  $\gamma$  being a constant.

The incorporating of Eq. 6.1 in the relaxation program is, however, a little bit more tricky for the dynamical case, as the Hamiltonian will now change in time. In principle, the iterative procedure requires a new diagonalization of the Hamiltonian at each time step. We avoid this difficulty using the sudden approximation.

First, we approximate the flux  $\phi(t) = \gamma t$  by an adequate step function, in which the flux remains unchanged during a time interval  $\tau_m$  before it jumps instantaneously to the next step value. Further, we assume a slowly increasing magnetic flux so that  $\tau_m \gg \tau_p$ . Finally, the flux step is determined so that it corresponds to a translation of  $k$ -vector (Eq. 6.1) by  $\delta k = 2\pi/N$ . The last assumption avoids the diagonalization problem, because the Hamiltonian is the same after a shift of  $2\pi/N$ , due to the periodicity of the band defined by Eq. 4.15, i.e. we have

$$H(t + \tau_m) = H(t). \quad (6.4)$$

We note that this assumption is not really necessary, and one could choose any fraction of  $\delta k$  for the flux. If for example, the step is chosen to be  $\delta k/n$ , we have to diagonalize only the  $n$  corresponding Hamiltonians, which then define the coherent evolution in the respective time intervals. The procedure is repetitive after  $n\tau_m$ .

Now we can apply the sudden approximation. We assume that the Hamiltonian changes discontinuously from  $H = H_1$  for times  $t < 0$  to  $H = H_2$  for  $t > 0$ . The stationary solution in both time domains are obtained from

$$H_1 u_i = E_j u_j \quad \text{and} \quad H_2 v_k = E_k v_k, \quad (6.5)$$

where the  $u$ 's and  $v$ 's are complete orthonormal sets of functions. The general solutions can then be written

$$\Psi_1(t < 0) = \sum_j a_j u_j \exp(-iE_j t/\hbar) \quad (6.6)$$

$$\Psi_2(t > 0) = \sum_k b_k v_k \exp(-iE_k t/\hbar), \quad (6.7)$$

where the coefficients  $a$  and  $b$  are independent of time. Using the continuity of  $\Psi$  at  $t = 0$ , we multiply Equations 6.6 and 6.7 by  $v_k^*$  for a particular  $k$  and integrate over the spatial coordinates to find

$$b_k = \sum_j a_j \int v_k^* u_j. \quad (6.8)$$

Eq. 6.8 yields the relation between the solutions before and after the instantaneous jump in the Hamiltonian. Under our particular assumptions, the function sets  $u$  and  $v$  have the same elements. Therefore, the function set  $v$  can be obtained from the set  $u$  by a permutation of the indices, i.e  $v_k = u_j$ . In the one-electron picture of a loop with  $N$  sites the resulting index relation is given by

$$j = \text{Mod}(k + 1, N). \quad (6.9)$$

## 6.2 Bloch Oscillations in small two-electron loop systems

We consider two electrons with parallel spins in a loop with  $N$  electronic sites. First of all we study the coherent electronic transport of an isolated ring in the absence of the electron-electron interaction. At  $t = 0$ , the electrons are assumed to be in the ground state of the electronic system<sup>1</sup>. We switch on a time dependent magnetic field, so that the loop is threaded by the flux  $\phi(t) = \gamma t$ ,  $t > 0$ , with

$$\gamma = \frac{2\pi}{N\tau_m} \phi_0. \quad (6.10)$$

The current in the ring is calculated by means of Eq. 5.6 after each time interval  $\tau_m$ .

Fig. 6.1 shows the time dependence of the current in a loop with  $N = 10$  sites and for  $\tau_m = 10^6 \tau_0$ . The oscillations in the current correspond to Bloch oscillations and describe how the electrons travel through the band. The electrons are not subject to any interaction except the Pauli exclusion and they shift from one state to the adjacent state after each time interval  $\tau_m$ . The period of the oscillation is thus  $N\tau_m$ .

### 6.2.1 Effects of Electron-Electron Interaction

Switching on the Coulomb interaction between the electrons, we observe beats in the time dependence of the current. This behavior is shown in Fig. 6.2 for two

<sup>1</sup>The choice of the initial state has no qualitative effect on the results.

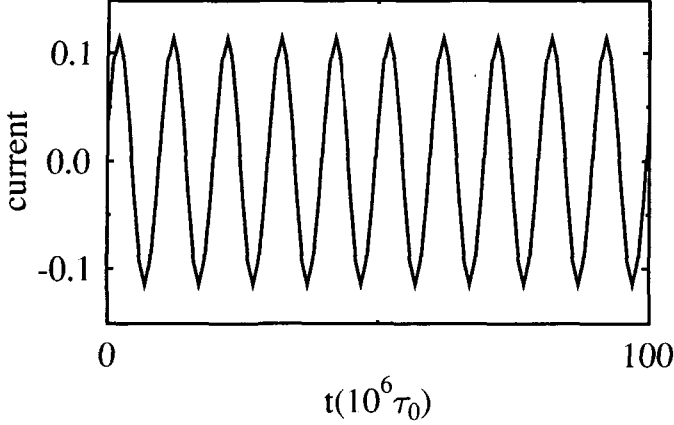


Figure 6.1: Bloch oscillations of the current for a fully coherent system of two electrons with parallel spins on a 1D loop with  $N = 10$  sites. No Coulomb interaction between the electrons is included. The increase of the flux with time is specified by  $\tau_m = 10^6 \tau_0$ .

electrons on a loop with  $N = 8$  sites threaded by the flux defined by the step time  $\tau_m = 10^5 \tau_0$ . The Coulomb interaction parameter is  $\alpha/R = 0.0001$  au.

Beats require the superposition of at least two different frequencies. In the present case, the first frequency can be identified as the frequency of the Bloch oscillations. The further frequencies depend on the electron-electron coupling, and describe the relative motion of the two electrons caused by the interaction. The period of these frequencies tends to infinity for vanishing Coulomb interaction.

Closer examination of the beat pattern in Fig. 6.2, shows that it is only approximately repetitive. In fact, an exact repetitive pattern can only be expected if the intervening frequencies are commensurable, which will in general not be the case.

In order to get a better understanding of the quantum beats in the presence of the electron-electron interaction, we have to recognize that the electron-electron interaction leads to a coupling between non-interacting two-electron basis states, whereas the current depends on the occupation of the states in the one-electron space. In the non-interacting case, the electrons travel through the band structure

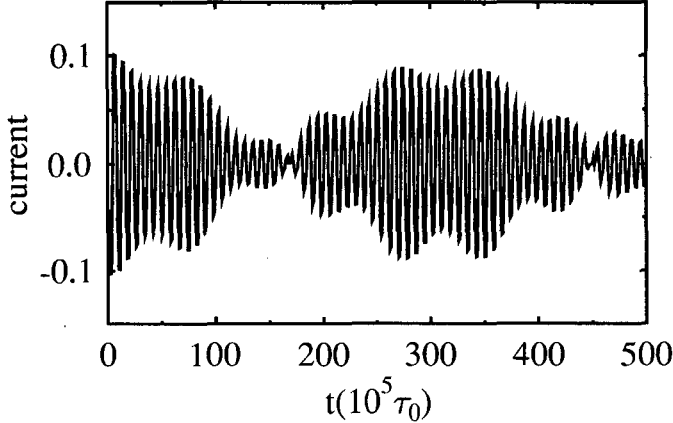


Figure 6.2: Bloch oscillations and quantum beats of the current for a fully coherent loop sample of two electrons with parallel spins, and with  $N = 8$  sites. The electron-electron interaction parameter is  $\alpha/R = 0.0001$  au and the increase of the flux with time is specified by  $\tau_m = 10^5 \tau_0$ .

according to equations 6.1 and 6.9, and the set of the occupation numbers  $\rho_e^{k(t)}$  in Eq. 5.6 remains unchanged. In the presence of the Coulomb interaction, the situation becomes different, since the coupling between the electrons depends on the electronic distribution  $\rho_e^{k(t)}$ , and it thus becomes time dependent. The resulting changes of the occupation  $\rho_e^{k(t)}$  give rise to the observed quantum beats.

We emphasize that the electron-electron interaction causes no dissipation, since it couples merely between different states of a *finite* electronic system. Though, the change in the oscillation pattern of the current might be very complicated, a direct current, which would indicate the existence of real dissipation, cannot be reached even for  $t \rightarrow \infty$ .

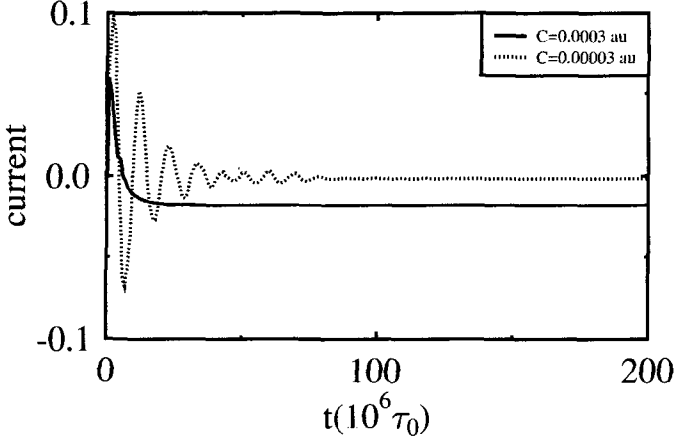


Figure 6.3: Damped Bloch oscillations for two electrons with parallel spin in a 1D loop with  $N = 10$  sites and for different electron-LVM couplings. The vibrational parameters are  $\omega = 0.01$  and  $\tau_p = 10^4 \tau_0$ . The system is driven with the same flux as in Fig. 6.1. The electron-electron interaction is set to zero ( $\alpha/R = 0$ ).

### 6.3 Damping of Bloch Oscillations and DC in Presence of Dissipation

We now introduce dissipation via coupling of the electronic states with a single local vibrational mode. We first consider two non-interacting electrons with parallel spins on a loop with  $N = 10$  sites. The band width parameter is  $\varepsilon = 0.06$  au. The single LVM is defined by  $\omega = 0.01$  au,  $\tau_p = 10^4 \tau_0$  and  $C = 3 \times 10^{-5}$  au for the dotted or  $C = 3 \times 10^{-4}$  au for the solid line. The increase of the flux with time is given by  $\tau_m = 10^6 \tau_0$ . Fig. 6.3 shows the time dependence of the current. We see that the Bloch oscillations for the weak coupling (dotted line) are damped and disappear after about 10 oscillations. A non-zero direct current is found for longer times. The amount of this direct current is independent of the initial state. However, it depends on the dissipation in the loop. We note that the norm of current increases, at first, with increasing electron-LVM coupling. Further increasing of the dissipation, however, suppresses the current.

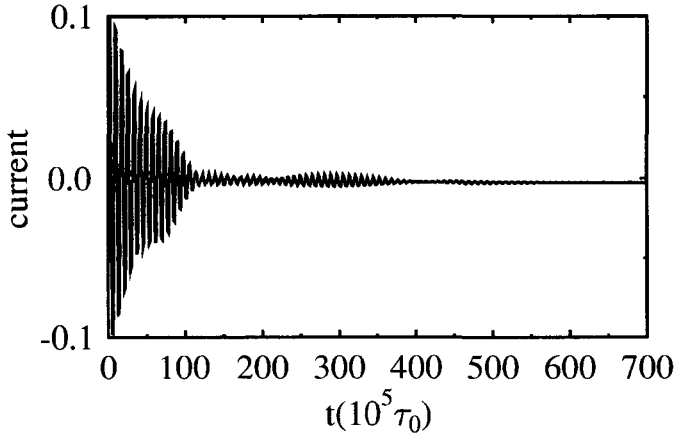


Figure 6.4: Dissipative transport of two electrons with parallel spin in the loop of Fig. 6.2. The vibrational parameters are  $\omega = 0.01$  au,  $\tau_p = 1000\tau_0$  and  $C = 3 \times 10^{-5}$ .

Similar behavior is seen for interacting electrons coupled to their environment. Fig. 6.4 shows the time dependence of the current for two electrons with parallel spins in the loop of Fig. 6.2. The electronic system is weakly coupled ( $C = 3 \times 10^{-5}$  au) to a single LVM, defined by  $\omega = 0.01$  au and  $\tau_p = 1000\tau_0$ . Weak beats can be seen before the current becomes dc.



## Chapter 7

# Conclusions

---

In this work we have been concerned with the physics of small sample systems and with the influence of the environment on their electronic properties. Our first objective was to clarify the origins of recent experimental results, such as the saturation of the phase-coherence time at low temperatures and the observation of nonuniversal conductance steps in clean quantum wires. These observations were previously not fully understood. Furthermore, a simple relaxation model is developed in order to achieve a microscopic understanding of the interplay between the environment and the sample.

Applying a phenomenological model based on the Landauer picture of dc transport, we have shown that these puzzling experimental results may both have the same origin. The openness of the electronic system has to be considered in either of both cases, when discussing the transport properties of the sample systems. The historical development in the case of conductance steps, i.e. from universal to nonuniversal behavior, is in fact a hint, that the coupling of the system to the environment is a crucial element to understand this effect. The nonuniversal conductance steps have been observed in quantum wires, which in contrast with previous ones were of a very high quality. In this case, electrons in the sample region can easily diffuse away.

The measured features of a mesoscopic sample depend considerably on its coupling to the outside. This is quite expected, since effects due to the quantum coherence of carriers are sensitively affected by the environment. Thus, more information about the contacts is needed to interpret properly the experimental data.

We have developed a simple numerical method to describe the time evolution of the density matrix of a finite small electronic system, which interacts with the environment merely via local vibrational modes. Our procedure, fully detailed in Chapter 4, takes into account the influence of the further environment by assuming phenomenologically a finite lifetime for these modes. In view of the results

obtained, we deduce that our approach is expedient to investigate electronic properties of small sample systems. In particular, we have applied our method to study the electronic relaxation in small 1D loops. We have found that weak electron-electron interactions facilitate the relaxation. Furthermore, we have shown that the final stationary state of the relaxed electronic sample system may be different from its ground state. The coupling to the environment is at the origin of these relaxation bottlenecks. The more adjacent states at the bottom of the conduction band approach each other, the more it becomes difficult for the relaxing sample system to reach the ideal ground state of the isolated sample.

Within our approach, we have studied persistent currents in a single 1D loop, which is threaded by a constant magnetic flux. In Chapter 5, we have shown that persistent currents in a relaxing sample system may be affected by the coupling to the environment. A ground state theory cannot be universally applied, since electron relaxation in a sample depends essentially on the local modes, which couple to the further environment. The contribution of the excited states to the persistent currents leads to higher harmonics in the current periodicity. In agreement with the results mentioned above, we have also found that the persistent currents of a relaxing sample approach their ground state values by increasing electron-electron interactions, as long as these are weak enough. Strong Coulomb interactions suppress the currents in a limited band at any flux value.

We have extended our study of the 1D loops in magnetic fields to the case of a time-dependent flux in Chapter 6. The currents driven by the corresponding electromotoric force have been investigated for different cases. Bloch oscillations of the current occur for non-interacting electrons in a fully coherent system. We have found additional quantum beats, when the Coulomb interaction is switched on. These beats are a result of the superposition of Bloch oscillations and of the relative motion of the electrons, which results itself from the Coulomb interaction. In the presence of weak dissipation, Bloch oscillations and quantum beats are damped. A direct current, whose value is independent of the initial state, is found for longer times.

A number of fundamental issues still deserve further study. In particular, it remains an experimental challenge to control the coupling parameters of the sample to its environment and to determine the influence of the latter on the outcome of the measurement. For the low-temperature saturation of the phase coherence as well as for the nonuniversal conductance steps we have made clear predictions, which could thence be verified experimentally. From the theoretical point of view we are just at the inception. The presented simple numerical approach is not elaborated enough to apply it to samples of realistic mesoscopic dimensions. The numerical efficiency can be improved by treating the problem in second order

perturbation theory in the interaction picture. Furthermore, in addition to the here-assumed electron-phonon interaction, one may also account for other relevant quantum mechanical couplings, which can mediate the interaction with a statistical environment. We note that our model description does not rely on the choice of a single lifetime parameter  $\tau_p$ . For example, one could easily extend it to treat a distribution of lifetime values within a Monte Carlo approach.

We have discussed two different ways to generate current. On the one hand, we have extended the dc transport picture, in which coherent and dissipative regions are properly separated, towards a more realistic one by allowing for the same processes in the sample as well as in the reservoirs. On the other hand, we have studied the dissipative direct current generation in a homogeneous loop system, in which dissipative processes occur everywhere with the same probability. Both approaches should become comparable by adding a strong dissipative “reservoir region” to a large loop system.



# Appendix A

## Electronic Arrays

---

### A.1 Two-Electron States

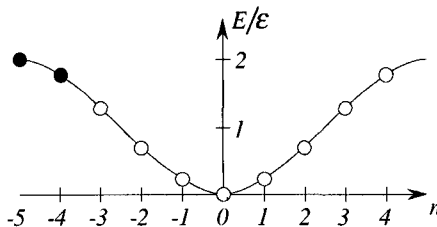
Our calculations for two electrons (in Chapters 4, 5 and 6) are performed introducing the electronic arrays that eventually account for the Pauli exclusion principle. The electronic states for a non-interacting system, defined by the tight-binding band Eq. 4.15 are shown in Fig. A.1 for  $N = 10$ , where two electrons occupy the states  $k_{-5} = -\pi$  and  $k_{-4} = -4\pi/5$ .

In order to specify all the possible non-interacting two-electron states in such a system we dispose of a vector array of the dimension  $(N(N - 1)/2) \times N$  for electrons with parallel spins

$$\begin{aligned}
 &|1, 1, 0 \dots, 0 \rangle \\
 &|1, 0, 1 \dots, 0 \rangle \\
 &\vdots \\
 &|0 \dots, 0, 1, 1 \rangle
 \end{aligned}
 \tag{A.1}$$

where the  $i$ -th position in each vector stands for  $k_i$  and the digit represents the occupation of the state. Speaking in terms of Bloch vectors Eq. 4.16 and Bloch

Figure A.1: Tight-binding band of a non-interacting electronic system with  $N = 10$  sites. The uppermost states for  $n = -5$  and  $n = -4$  are occupied.



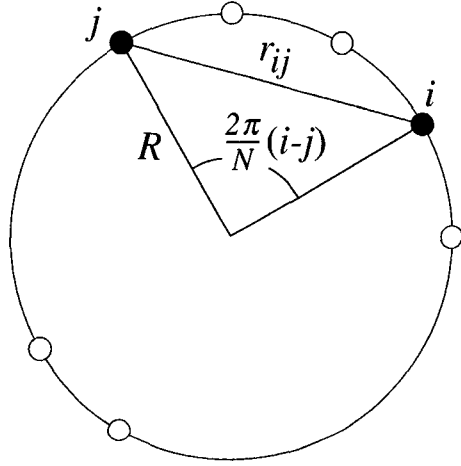


Figure A.2: The distance between the  $i$ -th and the  $j$ -th site on a 1D loop  $r_{ij}$

functions, the vector

$$|0 \dots, \underbrace{1}_{\mu} \dots, \underbrace{1}_{\nu} \dots, 0 \rangle \quad \text{for} \quad \mu \neq \nu \quad (\text{A.2})$$

represents in fact  $|\psi_{k_{\mu}}(\mathbf{r}_1), \psi_{k_{\nu}}(\mathbf{r}_2) \rangle$ .

Adding  $N$  more vectors

$$\begin{aligned} &|2, 0 \dots, 0 \rangle \\ &|0, 2 \dots, 0 \rangle \\ &\vdots \\ &|0 \dots, 0, 2 \rangle \end{aligned} \quad (\text{A.3})$$

to the array A.1 we describe the situation of electrons with opposite spins.

The Pauli exclusion is already included in A.1, as there is no case of double occupation in a state. However, the antisymmetry of the wavefunction has to be accounted for explicitly, when the electrons interact via the Coulomb interaction.

## A.2 Calculation of Electron-Electron Interaction on Loops

The Coulomb potential between two electrons with parallel spins on a loop in Fig. A.2 depends on their distance

$$v(\mathbf{r}_i, \mathbf{r}_j) = \frac{e^2}{r_{ij}}, \quad (\text{A.4})$$

with

$$r_{ij} = 2R \left| \sin\left(\frac{\pi(i-j)}{N}\right) \right| \quad (\text{A.5})$$

The Hamiltonian of the interaction can then be written as

$$H_{ee} = \frac{1}{2} \sum_{i \neq j}^N \sum_{i \neq j}^N \frac{e^2}{r_{ij}}. \quad (\text{A.6})$$

We resume all the constants, also the ones due to the choice of Rydberg atomic units of energy, together and replace them by  $\alpha$  to find

$$H_{ee} = \frac{\alpha}{R} \sum_{i \neq j}^N \sum_{i \neq j}^N \frac{1}{|\sin(\delta(i-j))|} \quad \text{with} \quad \delta = \frac{\pi}{N}. \quad (\text{A.7})$$

The matrix elements of the electron-electron interaction between the states  $|\psi_{k_\mu}(\mathbf{r}_1), \psi_{k_\nu}(\mathbf{r}_2) \rangle$  and  $|\psi_{k_\kappa}(\mathbf{r}_1), \psi_{k_\lambda}(\mathbf{r}_2) \rangle$  with respect to the antisymmetry can then be evaluated over

$$\begin{aligned} H_{ee}^{k_\mu k_\nu \rightarrow k_\kappa k_\lambda} = & \langle \psi_{k_\mu}(\mathbf{r}_1), \psi_{k_\nu}(\mathbf{r}_2) | H_{ee} | \psi_{k_\kappa}(\mathbf{r}_1), \psi_{k_\lambda}(\mathbf{r}_2) \rangle - \\ & \langle \psi_{k_\mu}(\mathbf{r}_2), \psi_{k_\nu}(\mathbf{r}_1) | H_{ee} | \psi_{k_\kappa}(\mathbf{r}_1), \psi_{k_\lambda}(\mathbf{r}_2) \rangle - \\ & \langle \psi_{k_\mu}(\mathbf{r}_1), \psi_{k_\nu}(\mathbf{r}_2) | H_{ee} | \psi_{k_\kappa}(\mathbf{r}_2), \psi_{k_\lambda}(\mathbf{r}_1) \rangle + \\ & \langle \psi_{k_\mu}(\mathbf{r}_2), \psi_{k_\nu}(\mathbf{r}_1) | H_{ee} | \psi_{k_\kappa}(\mathbf{r}_2), \psi_{k_\lambda}(\mathbf{r}_1) \rangle. \end{aligned} \quad (\text{A.8})$$

For example the first term on the right hand side of Eq. A.8 is given by

$$\langle \psi_{k_\mu}(\mathbf{r}_1), \psi_{k_\nu}(\mathbf{r}_2) | H_{ee} | \psi_{k_\kappa}(\mathbf{r}_1), \psi_{k_\lambda}(\mathbf{r}_2) \rangle = \frac{\alpha}{R} \sum_{m \neq n}^N \sum_{m \neq n}^N \frac{\exp(2i(k_\kappa - k_\mu)m\delta) \exp(2i(k_\lambda - k_\nu)n\delta)}{|\sin(\delta(m-n))|}. \quad (\text{A.9})$$



# Bibliography

---

- [1] R. Landauer, Electrical resistance of disordered one-dimensional lattices, *Philos. Mag.* **21**, 863 (1970).
- [2] D. J. Thouless, *J. Phys. C* **6**, L49 (1973).
- [3] D. J. Thouless, Maximum metallic resistance in thin wires, *Phys. Rev. Lett.* **39**, 1167 (1977).
- [4] E. Abrahams, P. W. Anderson, D. C. Licciardello, and T. V. Ramakrishnan, Scaling Theory of Localization: Absence of Quantum Diffusion in Two Dimensions, *Phys. Rev. Lett.* **42**, 673 (1979).
- [5] H. Haug and S. W. Koch, in *Quantum Theory of the Optical and Electronic Properties of Semiconductors*, 3rd ed. (World Scientific, Singapore, 1994).
- [6] T. Meyer, P. Thomas, and S. W. Koch, Coherent Effects in Photoexcited Semiconductor Superlattices with Electric Fields, *Phys. Low-Dim. Struct.* **3/4**, 1 (1998).
- [7] L. V. Keldysh, *Zh. Eksp. Teor. Fiz.* **47**, 1515 (1964).
- [8] W. Pötz, Microscopic theory of coherent carrier dynamics and phase breaking in semiconductors, *Phys. Rev. B* **54**, 5647 (1996).
- [9] S. Datta, *J. Phys.: Condens. Matter* **2**, 8023 (1990).
- [10] M. Büttiker, Role of quantum coherence in series resistors, *Phys. Rev. B* **33**, 3020 (1986).
- [11] K. Maschke and M. Schreiber, Unified description of coherent and dissipative electron transport, *Phys. Rev. B* **44**, 3835 (1991).
- [12] K. Maschke and M. Schreiber, Electron transport along a spatially disordered chain in the presence of dissipation, *Phys. Rev. B* **49**, 2295 (1994).
- [13] F. Gagel and K. Maschke, Influence of dissipation on quantum Hall plateaus, *Phys. Rev. B* **54**, 13885 (1996).
- [14] B. Altshuler, A. Aronov, and D. Khmelintski, Effects of electron-electron collisions with small energy on quantum localisation, *J. Phys. C* **15**, 7367 (1982).
- [15] P. Mohanty, E. Jariwala, and R. Webb, Intrinsic decoherence in mesoscopic systems, *Phys. Rev. Lett.* **78**, 3366 (1997).
- [16] A. Yacoby *et al.*, Nonuniversal Conductance Quantization in Quantum Wires, *Phys. Rev. Lett.* **77**, 4612 (1996).

- 
- [17] B. N. Murdin *et al.*, Direct observation of the LO phonon bottleneck in wide GaAs/Al<sub>x</sub>Ga<sub>1-x</sub>As quantum wells, *Phys. Rev. B* **55**, 5171 (1997).
  - [18] B. N. Murdin *et al.*, Suppression of LO phonon scattering in Landau quantized quantum dots, *Phys. Rev. B* **59**, R7817 (1999).
  - [19] G. Wang *et al.*, Time-resolved optical characterisation of InGaAs/GaAs quantum dots, *Appl. Phys. Lett.* **64**, 2815 (1994).
  - [20] N. Bohr, *Nature* **121**, 580 (1928).
  - [21] W. H. Zurek, Pointer basis of quantum apparatus, *Phys. Rev. D* **24**, 1516 (1981).
  - [22] H. D. Zeh, *Found Phys.* **1**, 69 (1970).
  - [23] Y. Imry, Decoherence in mesoscopic systems, *Physica Scripta* **T76**, 171 (1998).
  - [24] W. H. Zurek, Decoherence and the transition from quantum to classical, *Physics Today* **44**, 36 (1991).
  - [25] Y. Aharonov and D. Bohm, *Phys. Rev.* **115**, 485 (1959).
  - [26] A. Stern, Y. Aharonov, and Y. Imry, Phase uncertainty and loss of interference: A general picture, *Phys. Rev. A* **41**, 3436 (1990).
  - [27] R. Landauer, Electrical transport in open and closed systems, *Z. Phys. B* **68**, 217 (1987).
  - [28] G. Burmeister and K. Maschke, Scattering by time-periodic potentials in one dimension and its influence on electronic transport, *Phys. Rev. B* **57**, 13050 (1998).
  - [29] H. M. Pastawski, Classical and quantum transport from generalized Landauer-Büttiker equations, *Phys. Rev. B* **44**, 6329 (1991).
  - [30] R. Landauer, Conductance from Transmission: Common Sense Points, *Phys. Scr.* **T42**, 110 (1992).
  - [31] F. P. Milliken *et al.*, Effect of partial phase coherence on Aharonov-Bohm oscillations in metal loops, *Phys. Rev. B* **36**, 4465 (1987).
  - [32] D. P. DiVincenzo and C. L. Kane, Voltage fluctuations in mesoscopic metal rings and wires, *Phys. Rev. B* **38**, 3006 (1988).
  - [33] Ç. Kurdak, A. M. Chang, A. Chin, and T. Y. Chang, Quantum interference effects and spin-orbit interaction in quasi-one-dimensional wires and rings, *Phys. Rev. B* **46**, 6846 (1992).
  - [34] C. Beenakker and H. van Houten, Boundary scattering and weak localization of electrons in a magnetic field, *Phys. Rev. B* **38**, 3232 (1988).
  - [35] C. Beenakker and H. van Houten, *Solid State Phys.* **44**, 1 (1991).
  - [36] B. Altshuler, Fluctuations in the extrinsic conductivity of disordered conductors, *Pis'ma Zh. Eksp. Teor. Fiz.* **41**, 530 (1985).
  - [37] P. Lee, A. Stone, and H. Fukuyama, Universal conductance fluctuations in metals: Effects of finite temperature, interactions, and magnetic field, *Phys. Rev. B* **35**, 1039 (1987).

- [38] S. Washburn and R. Webb, Rep. Prog. Phys. **55**, 1311 (1992).
- [39] M. Sonck and M. Wagner, Coherence tendencies in the transport of translationally invariant exciton-phonon systems, Phys. Rev. B **54**, 9213 (1996).
- [40] J. A. Katine, M. J. Berry, R. M. Westervelt, and A. C. Gossard, Determination of the electronic phase coherence time in one-dimensional channels, Phys. Rev. B **57**, 1698 (1998).
- [41] J. P. Bird *et al.*, Phase breaking in ballistic quantum dots: Transition from two- to zero-dimensional behavior, Phys. Rev. B **51**, 18037 (1995).
- [42] K. Hecker, H. Hegger, A. Altland, and K. Fiegle, Conductance fluctuations in mesoscopic normal-metal/ superconductor samples, Phys. Rev. Lett. **79**, 1547 (1997).
- [43] P. Mohanty and R. Web, Decoherence and quantum fluctuations, Phys. Rev. B **55**, R13 452 (1997).
- [44] D. S. Gloubev and A. D. Zaikin, Quantum Decoherence in Disordered Mesoscopic Systems, Phys. Rev. Lett. **81**, 1074 (1998).
- [45] D. S. Gloubev and A. D. Zaikin, Quantum decoherence and weak localization at low temperatures, Phys. Rev. B **59**, 9195 (1999).
- [46] Y. B. Khavin, M. E. Gershenson, and A. L. Bogdanov, Decohorence and the Thouless Crossover in One-Dimensional Conductors, Phys. Rev. Lett. **81**, 1066 (1998).
- [47] N. Lang, Anomalous dependence of resistance on length in atomic wires, Phys. Rev. Lett. **79**, 1357 (1997).
- [48] S. Datta *et al.*, Current-Voltage Characteristics of Self-Assembled Monolayers by Scanning Tunneling Microscopy, Phys. Rev. Lett. **79**, 2530 (1997).
- [49] B. L. A. *et al.*, in *Soviet Scientific Reviews. Section A: Physics Reviews*, edited by I. M. Khalatnikov (Howard Academic, New York, 1987), Vol. 9.
- [50] J. J. Lin and N. Giordano, Localization and electron-electron effects in thin Au-Pd films and wires, Phys. Rev. B **35**, 545 (1987).
- [51] B. J. van Wees *et al.*, Quantized conductance of point contacts in a two-dimensional electron gas, Phys. Rev. Lett. **60**, 848 (1988).
- [52] J. L. Costa-Krämer, N. García, P. García-Mochales, and P. A. Serena, Surf. Sci. Lett. **342**, L1144 (1995).
- [53] R. J. Haug, Semicond. Sci. Technol. **9**, 131 (1993).
- [54] M. Rother, W. Wegscheider, M. Bichler, and G. Abstreiter, in *24th International Conference on The Physics of Semiconductors* (World Scientific, Singapore, 1998):
- [55] D. Kaufman *et al.*, Conductance quantization in V-groove quantum wires, Phys. Rev. B **59**, 10433 (1999).
- [56] A. Y. Alekseev and V. V. Cheianov, Nonuniversal conductance quantization in high-quality quantum wires, Phys. Rev. B **57**, R6834 (1998).
- [57] P. Supancic *et al.*, Transport analysis of the thermalization and energy relaxation of photoexcited hot electrons in Ge-doped GaAs, Phys. Rev. B **53**, 7785 (1996).

- [58] T. Kuhn and F. Rossi, Monte Carlo simulation of ultrafast processes in photoexcited semiconductors: Coherent and incoherent dynamics, *Phys. Rev. B* **46**, 7496 (1992).
- [59] S. Haas, F. Rossi, and T. Kuhn, Generalized Monte Carlo approach for the study of the coherent ultrafast carrier dynamics in photoexcited semiconductors, *Phys. Rev. B* **53**, 12855 (1996).
- [60] K. Schönhammer and C. Wöhler, Hot electron relaxation: Exact solution for a many-electron model, *Phys. Rev. B* **55**, 13564 (1997).
- [61] V. Meden, C. Wöhler, J. Fricke, and K. Schönhammer, Hot-electron relaxation: An exactly solvable model and improved quantum kinetic equations, *Phys. Rev. B* **52**, 5624 (1995).
- [62] K. Schönhammer, Confined coherence and analytic properties of Green's functions, *Phys. Rev. B* **58**, 3494 (1998).
- [63] F. Rossi, A. D. Carlo, and P. Luigi, Microscopic theory of Quantum-Transport Phenomena in Mesoscopic Systems: A Monte Carlo Approach, *Phys. Rev. Lett.* **80**, 3348 (1998).
- [64] F. Rossi, S. Haas, and T. Kuhn, Ultrafast Relaxation of Photoexcited Carriers: The Role of Coherence in the Generation Process, *Phys. Rev. Lett.* **72**, 152 (1994).
- [65] T. A. Brun, Quantum Jumps as Decoherent Histories, *Phys. Rev. Lett.* **78**, 1833 (1997).
- [66] F. Reuse, Introduction à l'électrodynamique et optique quantiques, in french, EPFL, lecture notes.
- [67] K. Houshangpour and K. Maschke, submitted to *Phys. Rev. B* (unpublished).
- [68] M. Büttiker, Y. Imry, and R. Landauer, Josephson behavior in small normal one-dimensional rings, *Phys. Lett. A* **96**, 365 (1983).
- [69] R. Landauer and M. Büttiker, Resistance of small metallic loops, *Phys. Rev. Lett.* **54**, 2049 (1985).
- [70] H.-F. Cheung, Y. Gefen, E. K. Riedel, and W.-H. Shih, Persistent currents in small one-dimensional metal rings, *Phys. Rev. B* **37**, 6050 (1988).
- [71] N. Trivedi and D. A. Browne, Mesoscopic ring in a magnetic field: Reactive and dissipative response, *Phys. Rev. B* **38**, 9581 (1988).
- [72] L. P. Lévy, G. Dolan, J. Dunsmuir, and H. Bouchiat, Magnetization of Mesoscopic Copper Rings: Evidence for Persistent Currents, *Phys. Rev. Lett.* **64**, 2074 (1990).
- [73] V. Chandrasekhar *et al.*, Magnetic Response of a Single, Isolated Gold Loop, *Phys. Rev. Lett.* **67**, 3578 (1991).
- [74] D. Mailly, C. Chapelier, and A. Benoit, Experimental Observation of Persistent Currents in a GaAs-AlGaAs Single Loop, *Phys. Rev. Lett.* **70**, 2020 (1993).
- [75] C. Kittel, in *Quantum Theory of Solids*, 4th ed. (John Wiley & Sons, Inc., New York, 1967), Chap. 9, p. 190.

- 
- [76] G. Burmeister, Coherent Electronic Transport in Time-Periodic Mesoscopic Systems, Ph.D. thesis, École Polytechnique Fédérale de Lausanne, 2000.
  - [77] G. Montambaux, H. Bouchiat, D. Sigeti, and R. Friesner, Persistent currents in mesoscopic rings: Ensemble average, *Phys. Rev. B* **42**, 7647 (1990).
  - [78] F. Bloch, *Z. Phys.* **52**, 555 (1928).
  - [79] C. Zener, *Proc. R. Soc. London Ser. A* **145**, 523 (1934).
  - [80] J. Feldmann *et al.*, Optical investigation of Bloch oscillations in a semiconductor superlattice, *Phys. Rev. B* **46**, 7252 (1992).
  - [81] C. Waschke *et al.*, Coherent Submillimeter Wave Emission from Bloch Oscillations in a Semiconductor Superlattice, *Phys. Rev. Lett.* **70**, 3319 (1993).
  - [82] T. Dekorsy, P. Leisching, K. Köhler, and H. Kurz, Electro-optic detection of Bloch oscillations, *Phys. Rev. B* **50**, 8106 (1994).

# Acknowledgements

---

I would very much like to thank the director of my thesis Dr. Klaus Maschke not only for all his scientific contributions and suggestions to this work, but also for all that he taught me during the past four years. In particular, his strong support during the daily ups and downs is most appreciated.

I would also thank Guido Burmeister for all the interesting discussions we had together. I fully appreciated his helps during our common “last-days-stress”.

Special thanks to my friends Rajesh Ambigapathy, Giovanni Cangiani, Caspar J. Fall, Fabio Favot and Thomas Maxisch for their helpful contributions to this manuscript. And to Andrea, Delphine, Michele, Christiano, Sabrina, Lynda, Barbara, Cécile, Ioannis, Alain, Francesco, Ouafa, David and Genia for making live easier. Thanks to the iranian community of the EPFL, especially to my dearest friends Omid “mido” Shojaei and Alireza Golshani for all the beautiful words we said to each other in our mother tongue.

I am very grateful and most honoured that Prof. F. Rossi, Prof. H. Beck and Prof. J.-Ph. Ansermet have accepted to be members of the jury. I would thank Dr. F. Reuse for his highly appreciated contributions to my understanding of quantum mechanics.

Last but not least, I am in debt to my family, who has always been extremely supportive during these long years of study regardless of the physical distance between us. To my mother, who sacrificed her life for her children, and to my father, whose memory gave me force.

## Curriculum Vitæ

Nom **Houshang Pour Islam**

Prénom **Kamran**

Né le 24 mai 1966

à Téhéran, Iran

Nationalité Iranienne

déc. 1995      Physicien diplômé de J. W. G. Universität, Frankfurt/Main, Allemagne

Travail de diplôme, intitulé *Debye-Waller Faktor und Mössbauer-Lamb Fraktion in mesoskopischen Kristallen*, réalisé sous la direction du Prof. L. Hirst

1989–1995      Etudes de Physique, J. W. von Goethe Universität, Frankfurt/Main, Allemagne

1984–1987      Etudes de Physique, Université de Téhéran, Téhéran, Iran